



Supplement of

Retrievals of tropospheric ozone profiles from the synergism of AIRS and OMI: methodology and validation

Dejian Fu et al.

Correspondence to: Dejian Fu (dejian.fu@jpl.nasa.gov)

The copyright of individual parts of the supplement might differ from the CC BY 4.0 License.

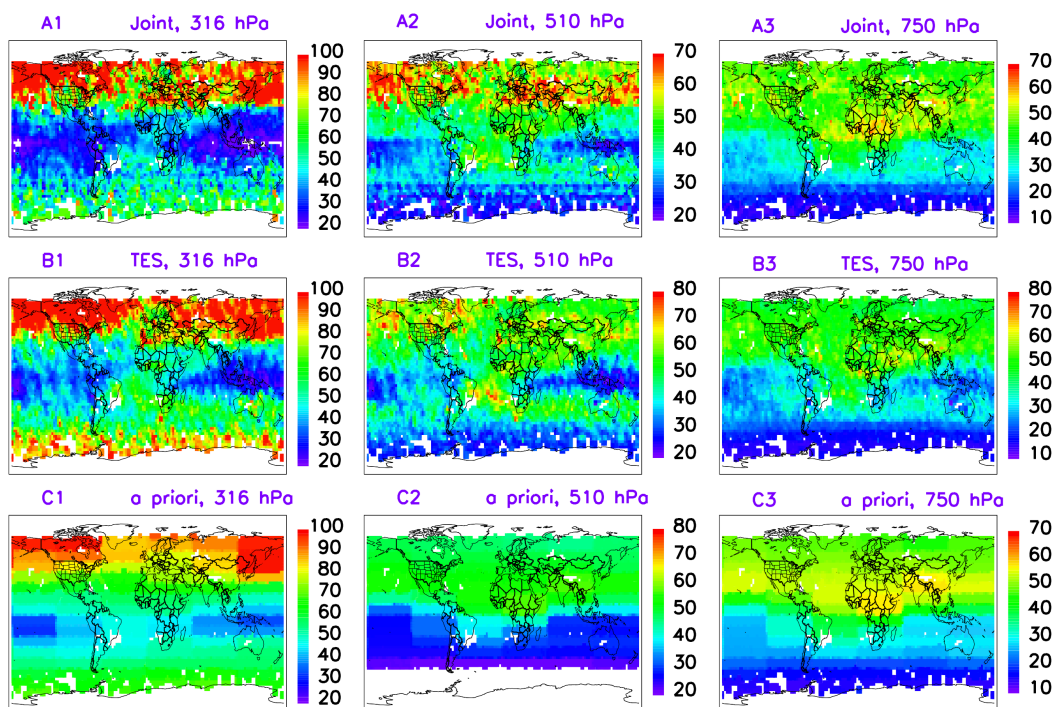


Figure S1: Global maps of monthly averaged ozone (O_3) volume mixing ratio (VMR) with a unit of ppb. The A-Train measurements in January 2006 were used in creating these global maps. Comparison of Joint AIRS+OMI (top row, A), TES (middle row, B), and a priori (bottom row C) ozone VMR for the pressure level of 316, 510 and 750 hPa (columns left, middle, right), respectively. All data have been gridded to $2.5^\circ \times 2.5^\circ$ cells.

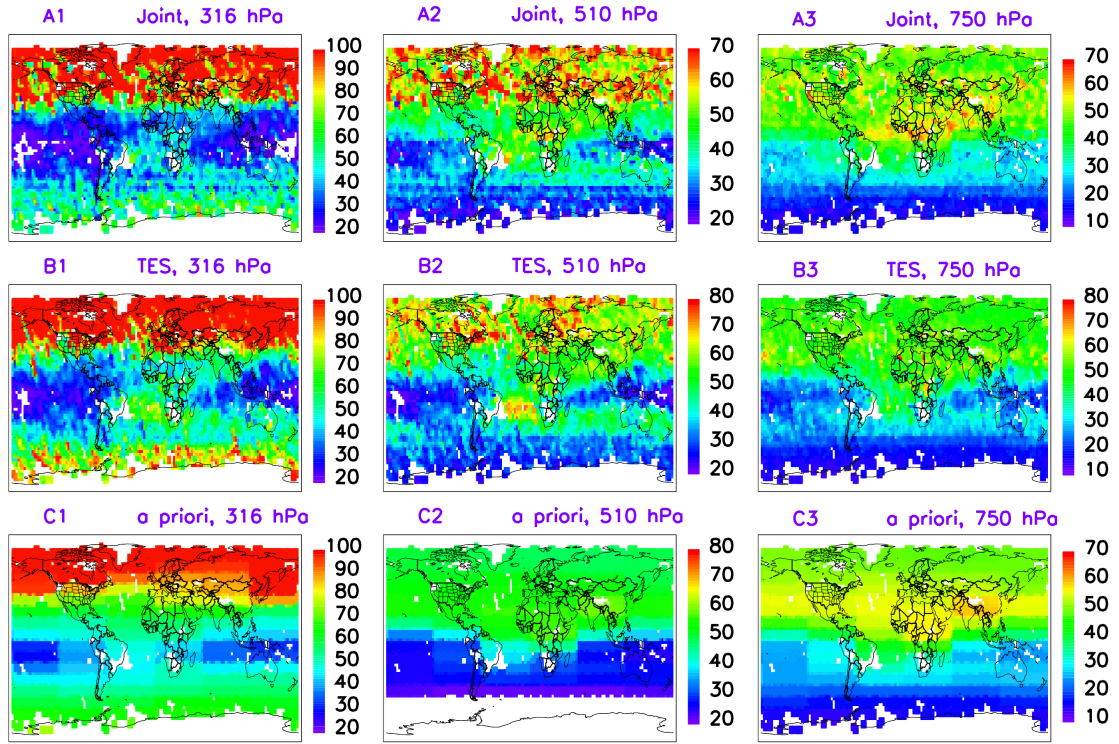


Figure S2: Global maps of monthly averaged ozone (O_3) volume mixing ratio (VMR) with a unit of ppb. The A-Train measurements in February 2006 were used in creating these global maps. Comparison of Joint AIRS+OMI (top row, A), TES (middle row, B), and a priori (bottom row C) ozone VMR for the pressure level of 316, 510 and 750 hPa (columns left, middle, right), respectively. All data have been gridded to $2.5^\circ \times 2.5^\circ$ cells.

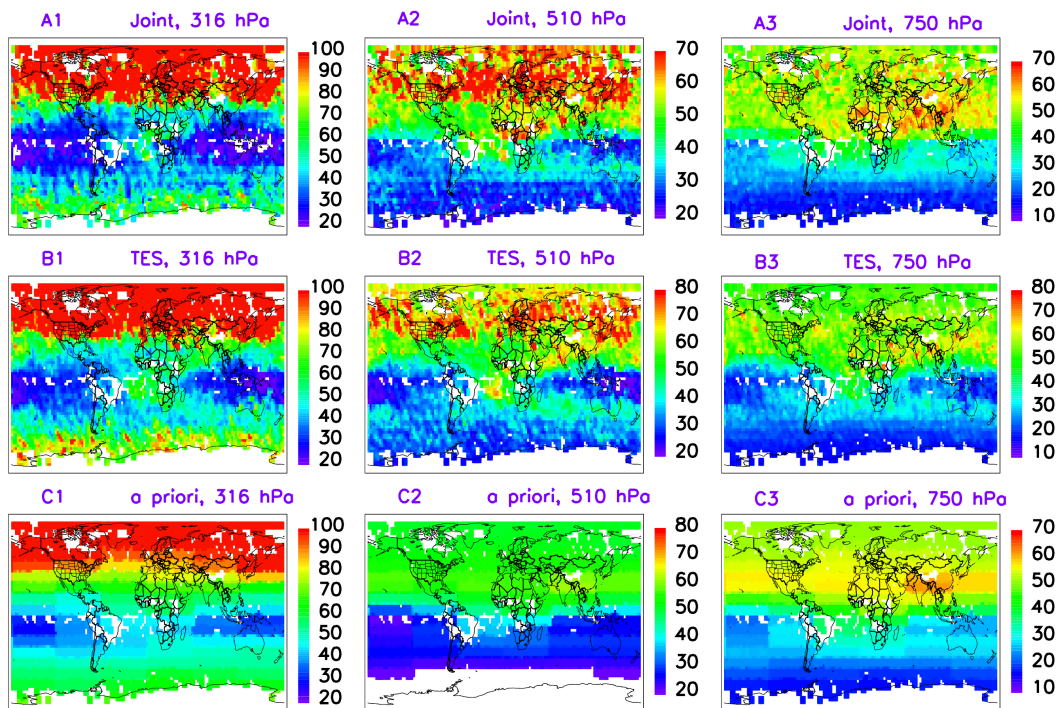


Figure S3: Global maps of monthly averaged ozone (O_3) volume mixing ratio (VMR) with a unit of ppb. The A-Train measurements in March 2006 were used in creating these global maps. Comparison of Joint AIRS+OMI (top row, A), TES (middle row, B), and a priori (bottom row C) ozone VMR for the pressure level of 316, 510 and 750 hPa (columns left, middle, right), respectively. All data have been gridded to $2.5^\circ \times 2.5^\circ$ cells.

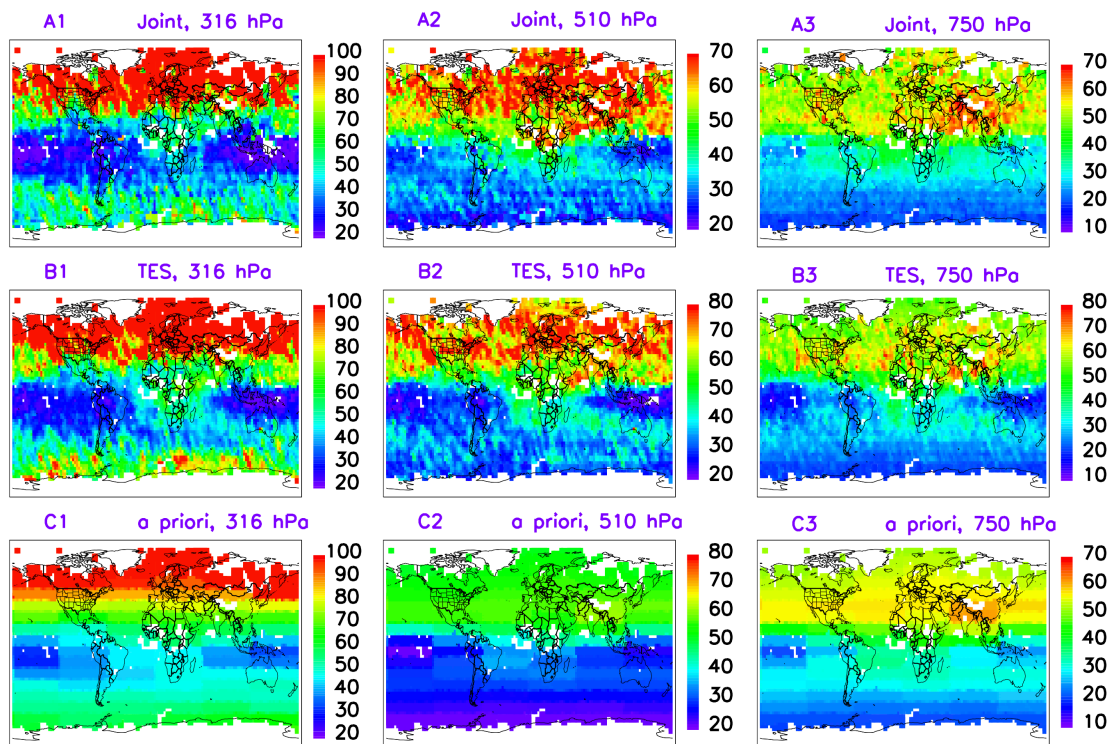


Figure S4: Global maps of monthly averaged ozone (O_3) volume mixing ratio (VMR) with a unit of ppb. The A-Train measurements in April 2006 were used in creating these global maps. Comparison of Joint AIRS+OMI (top row, A), TES (middle row, B), and a priori (bottom row C) ozone VMR for the pressure level of 316, 510 and 750 hPa (columns left, middle, right), respectively. All data have been gridded to $2.5^\circ \times 2.5^\circ$ cells.

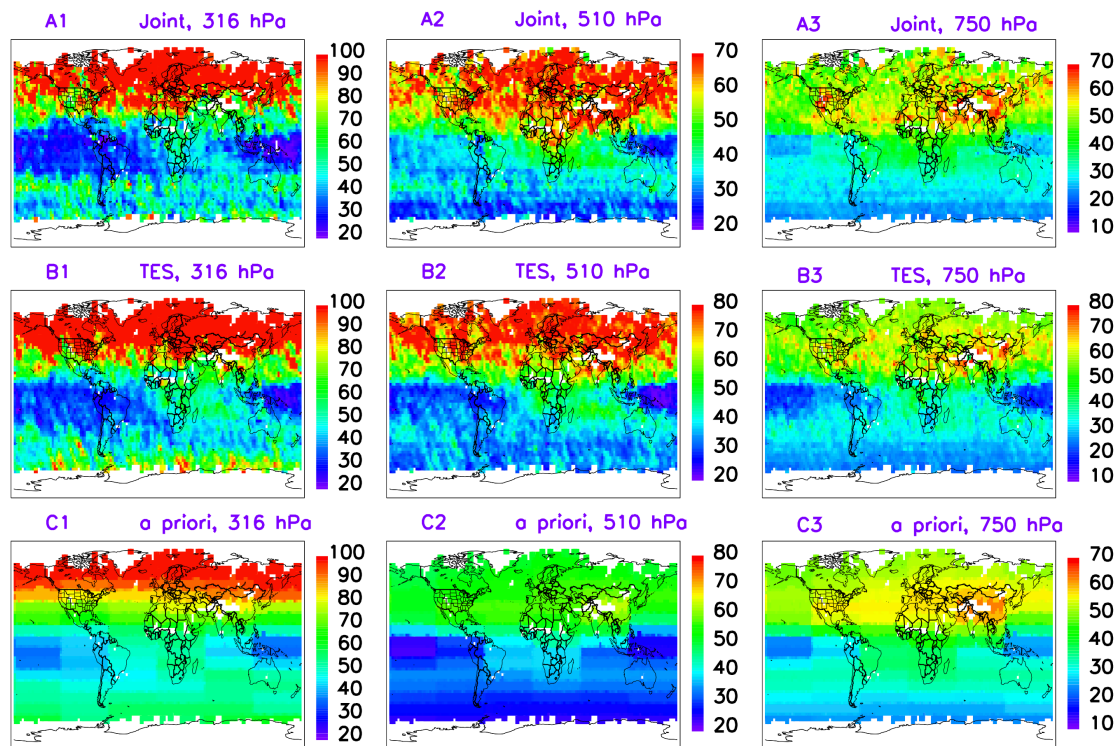


Figure S5: Global maps of monthly averaged ozone (O_3) volume mixing ratio (VMR) with a unit of ppb. The A-Train measurements in May 2006 were used in creating these global maps. Comparison of Joint AIRS+OMI (top row, A), TES (middle row, B), and a priori (bottom row C) ozone VMR for the pressure level of 316, 510 and 750 hPa (columns left, middle, right), respectively. All data have been gridded to $2.5^\circ \times 2.5^\circ$ cells.

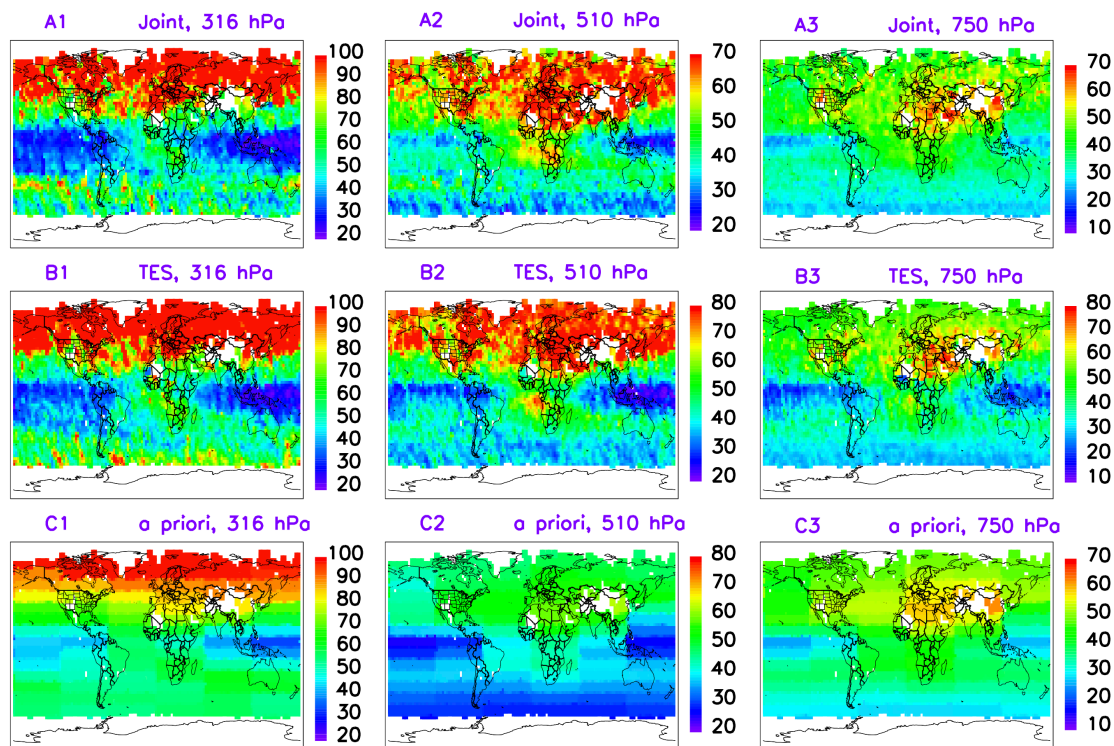


Figure S6: Global maps of monthly averaged ozone (O_3) volume mixing ratio (VMR) with a unit of ppb. The A-Train measurements in June 2006 were used in creating these global maps. Comparison of Joint AIRS+OMI (top row, A), TES (middle row, B), and a priori (bottom row C) ozone VMR for the pressure level of 316, 510 and 750 hPa (columns left, middle, right), respectively. All data have been gridded to $2.5^\circ \times 2.5^\circ$ cells.

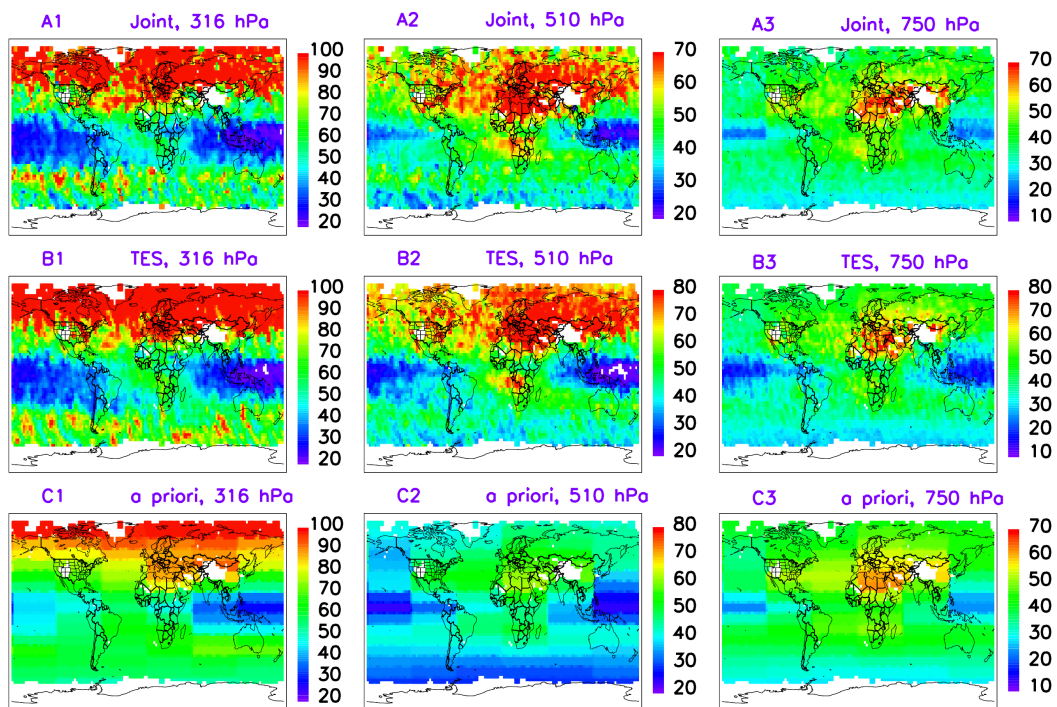


Figure S7: Global maps of monthly averaged ozone (O_3) volume mixing ratio (VMR) with a unit of ppb. The A-Train measurements in July 2006 were used in creating these global maps. Comparison of Joint AIRS+OMI (top row, A), TES (middle row, B), and a priori (bottom row C) ozone VMR for the pressure level of 316, 510 and 750 hPa (columns left, middle, right), respectively. All data have been gridded to $2.5^\circ \times 2.5^\circ$ cells.

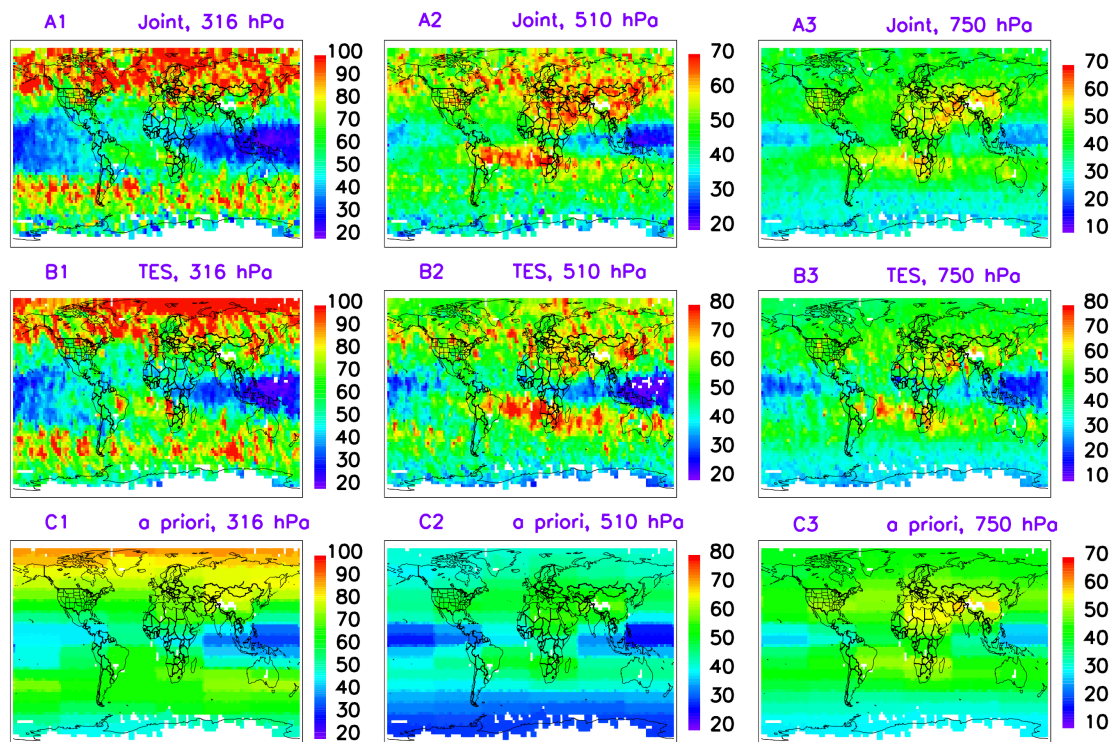


Figure S8: Global maps of monthly averaged ozone (O_3) volume mixing ratio (VMR) with a unit of ppb. The A-Train measurements in September 2006 were used in creating these global maps. Comparison of Joint AIRS+OMI (top row, A), TES (middle row, B), and a priori (bottom row C) ozone VMR for the pressure level of 316, 510 and 750 hPa (columns left, middle, right), respectively. All data have been gridded to $2.5^\circ \times 2.5^\circ$ cells.

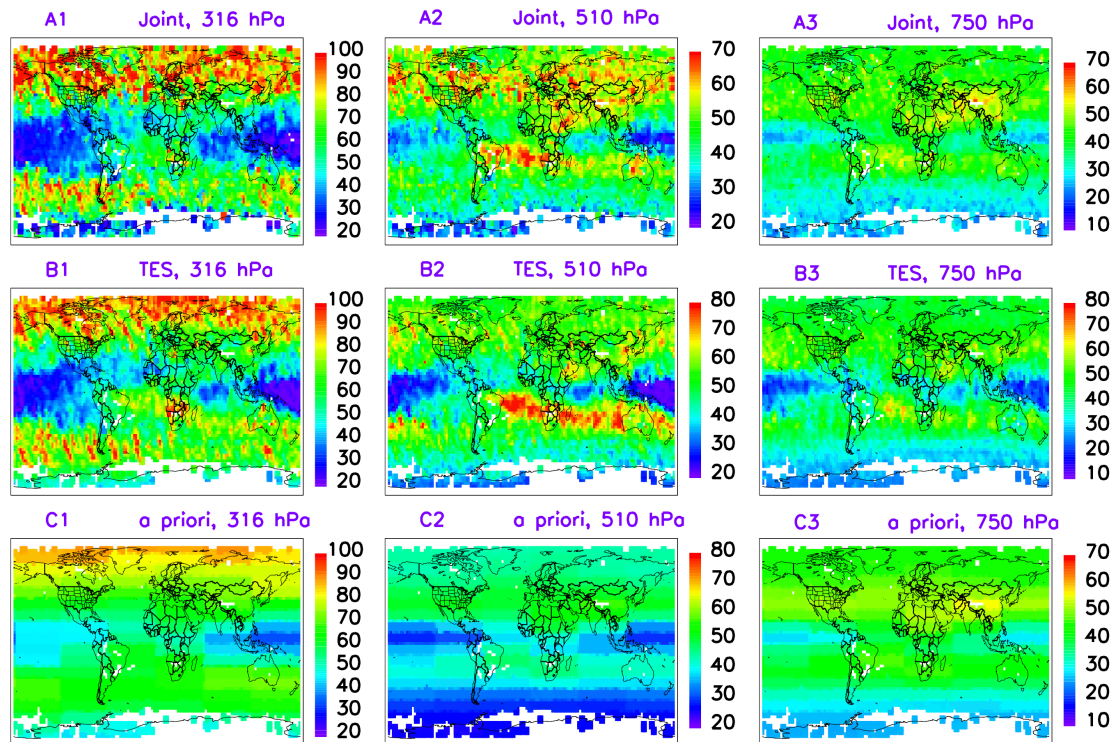


Figure S9: Global maps of monthly averaged ozone (O_3) volume mixing ratio (VMR) with a unit of ppb. The A-Train measurements in October 2006 were used in creating these global maps. Comparison of Joint AIRS+OMI (top row, A), TES (middle row, B), and a priori (bottom row C) ozone VMR for the pressure level of 316, 510 and 750 hPa (columns left, middle, right), respectively. All data have been gridded to $2.5^\circ \times 2.5^\circ$ cells.

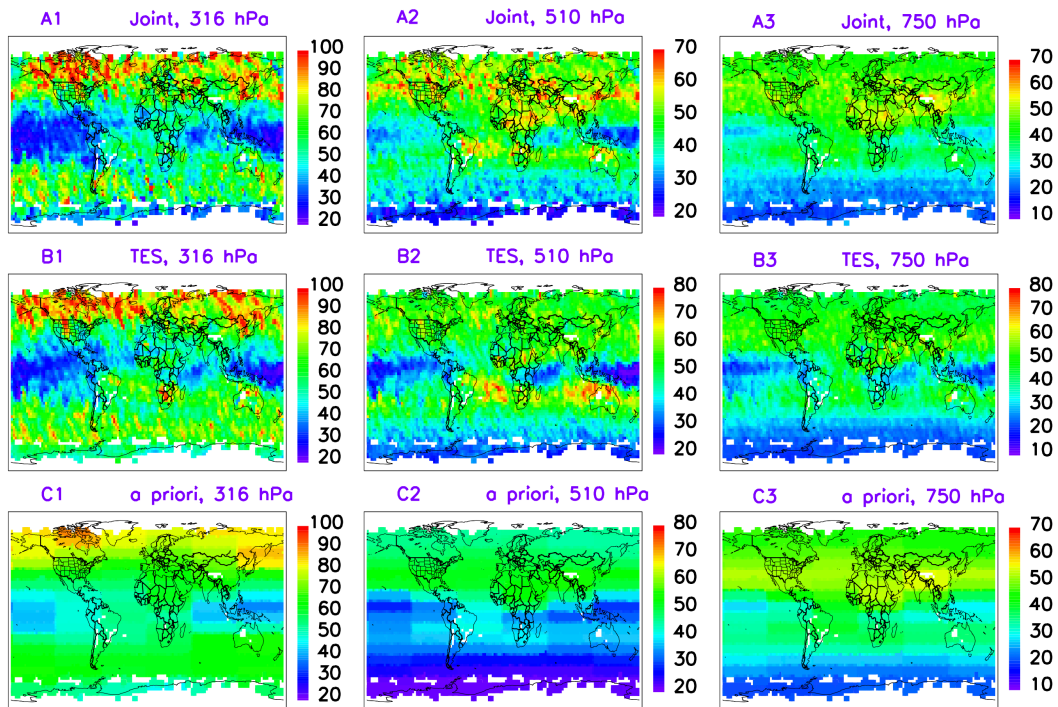


Figure S10: Global maps of monthly averaged ozone (O_3) volume mixing ratio (VMR) with a unit of ppb. The A-Train measurements in November 2006 were used in creating these global maps. Comparison of Joint AIRS+OMI (top row, A), TES (middle row, B), and a priori (bottom row C) ozone VMR for the pressure level of 316, 510 and 750 hPa (columns left, middle, right), respectively. All data have been gridded to $2.5^\circ \times 2.5^\circ$ cells.

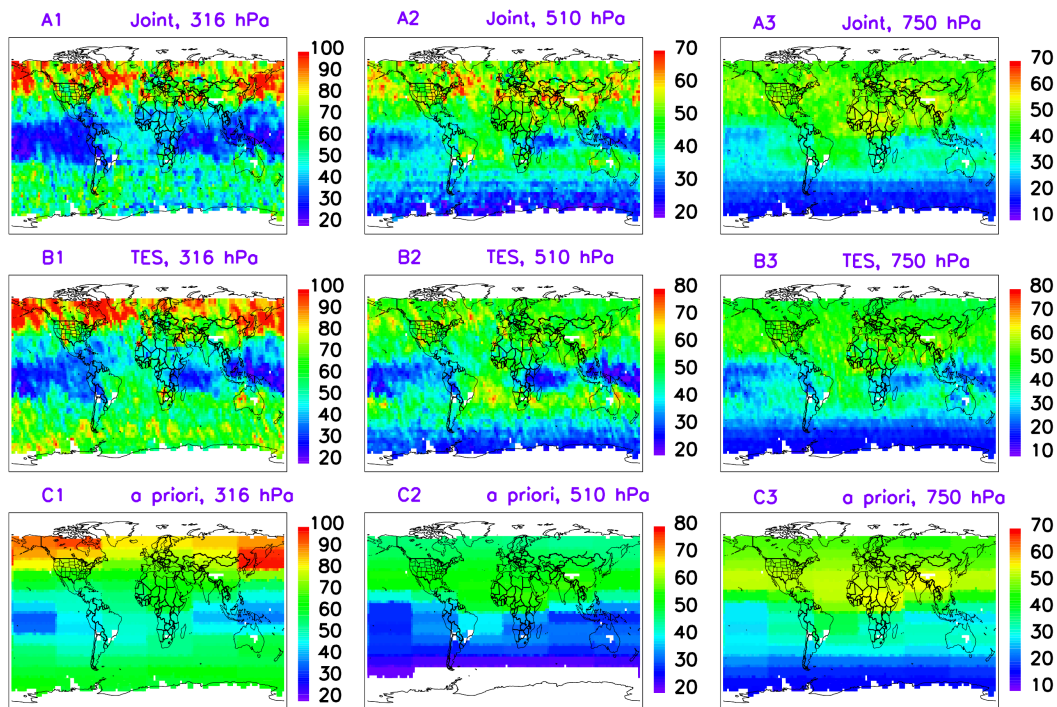


Figure S11: Global maps of monthly averaged ozone (O_3) volume mixing ratio (VMR) with a unit of ppb. The A-Train measurements in December 2006 were used in creating these global maps. Comparison of Joint AIRS+OMI (top row, A), TES (middle row, B), and a priori (bottom row C) ozone VMR for the pressure level of 316, 510 and 750 hPa (columns left, middle, right), respectively. All data have been gridded to $2.5^\circ \times 2.5^\circ$ cells.

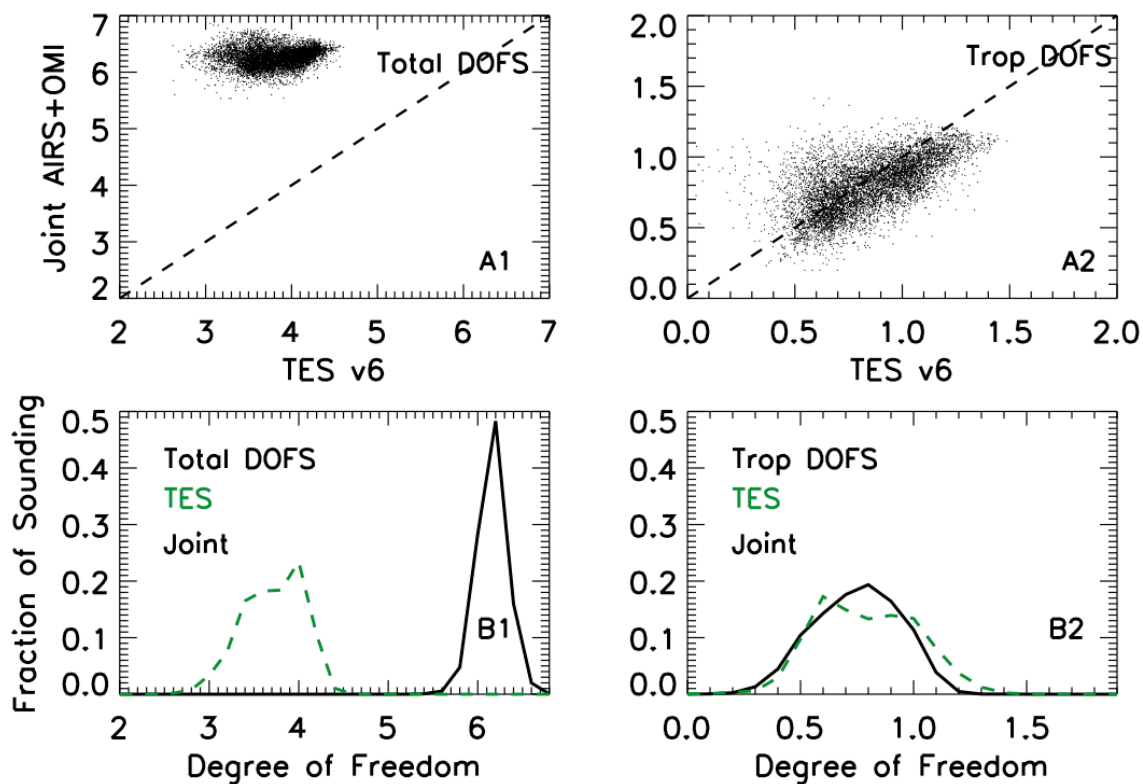


Figure S12: Degree of freedom of signals (DOFS) for January 2006 monthly mean O_3 over globe shown in Fig. S1. (A1) total DOFS; (A2) tropospheric DOFS; and (B1) histogram of total DOFS: joint AIRS+OMI (black line) and TES version 6 (green dash); (B2) histogram of tropospheric DOFS joint AIRS+OMI (black line) and TES version 6 (green dash).

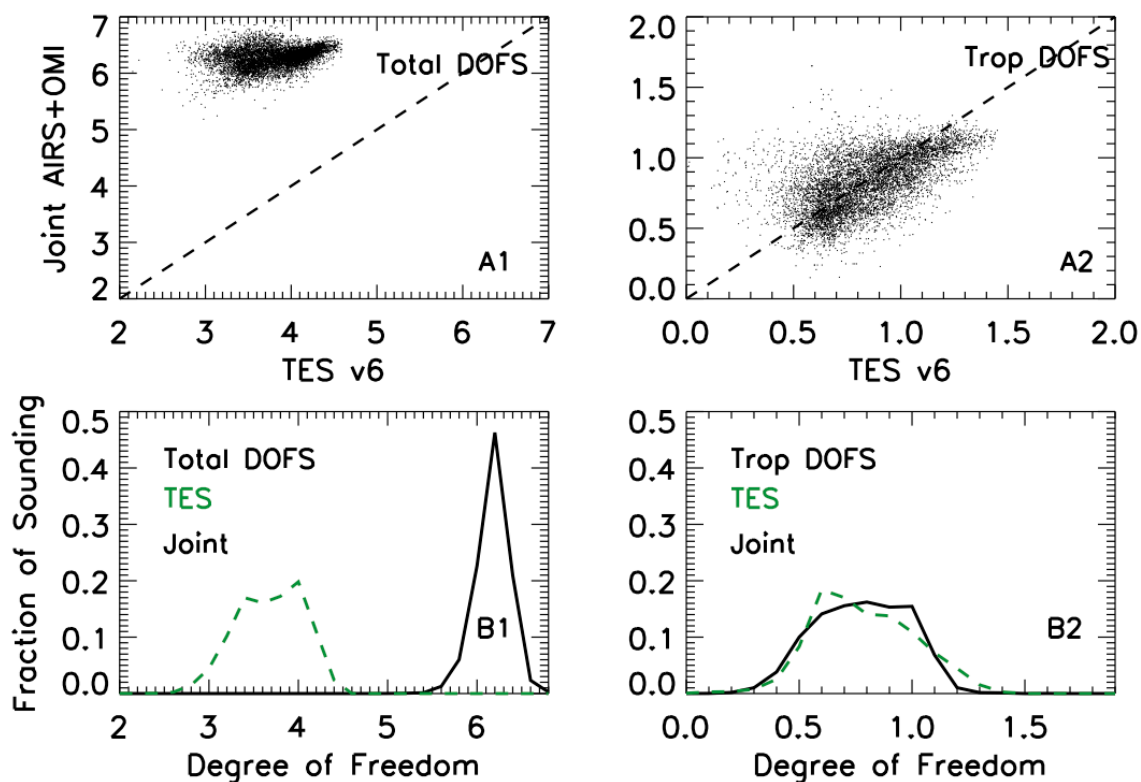


Figure S13: Degree of freedom of signals (DOFS) for February 2006 monthly mean O_3 over globe shown in Fig. S2. (A1) total DOFS; (A2) tropospheric DOFS; and (B1) histogram of total DOFS: joint AIRS+OMI (black line) and TES version 6 (green dash); (B2) histogram of tropospheric DOFS joint AIRS+OMI (black line) and TES version 6 (green dash).

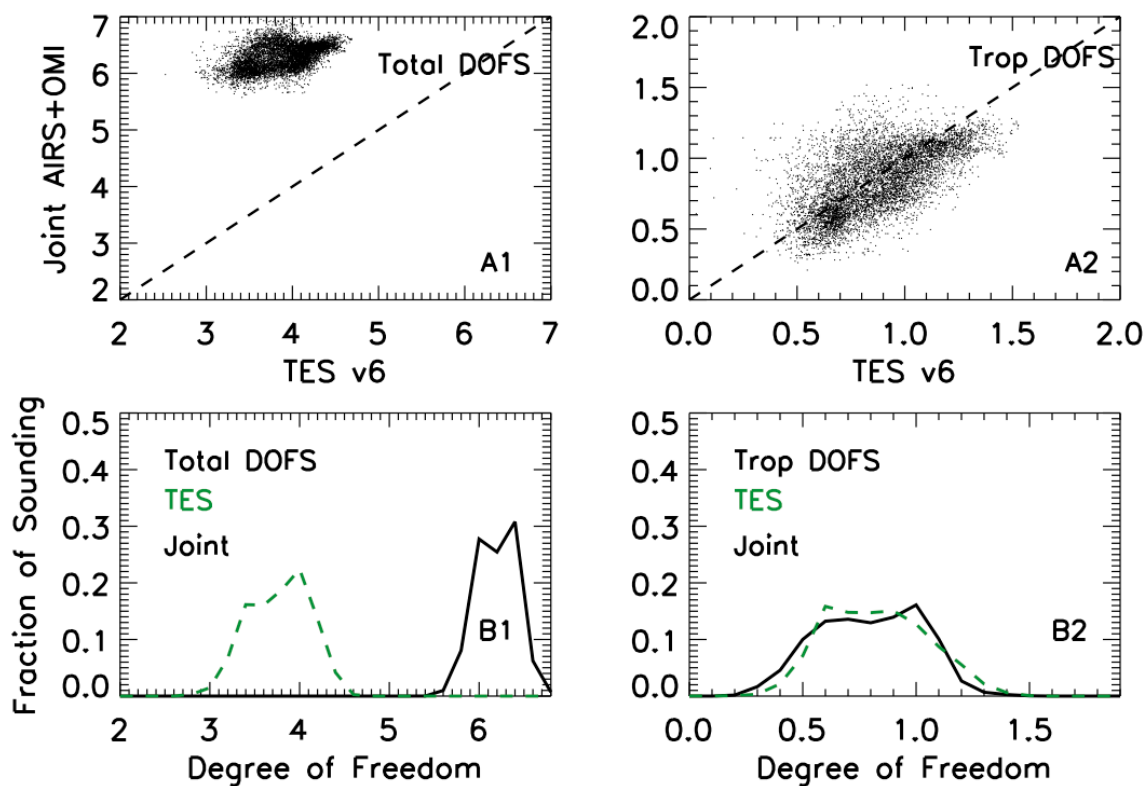


Figure S14: Degree of freedom of signals (DOFS) for March 2006 monthly mean O₃ over globe shown in Fig. S3. (A1) total DOFS; (A2) tropospheric DOFS; and (B1) histogram of total DOFS: joint AIRS+OMI (black line) and TES version 6 (green dash); (B2) histogram of tropospheric DOFS joint AIRS+OMI (black line) and TES version 6 (green dash).

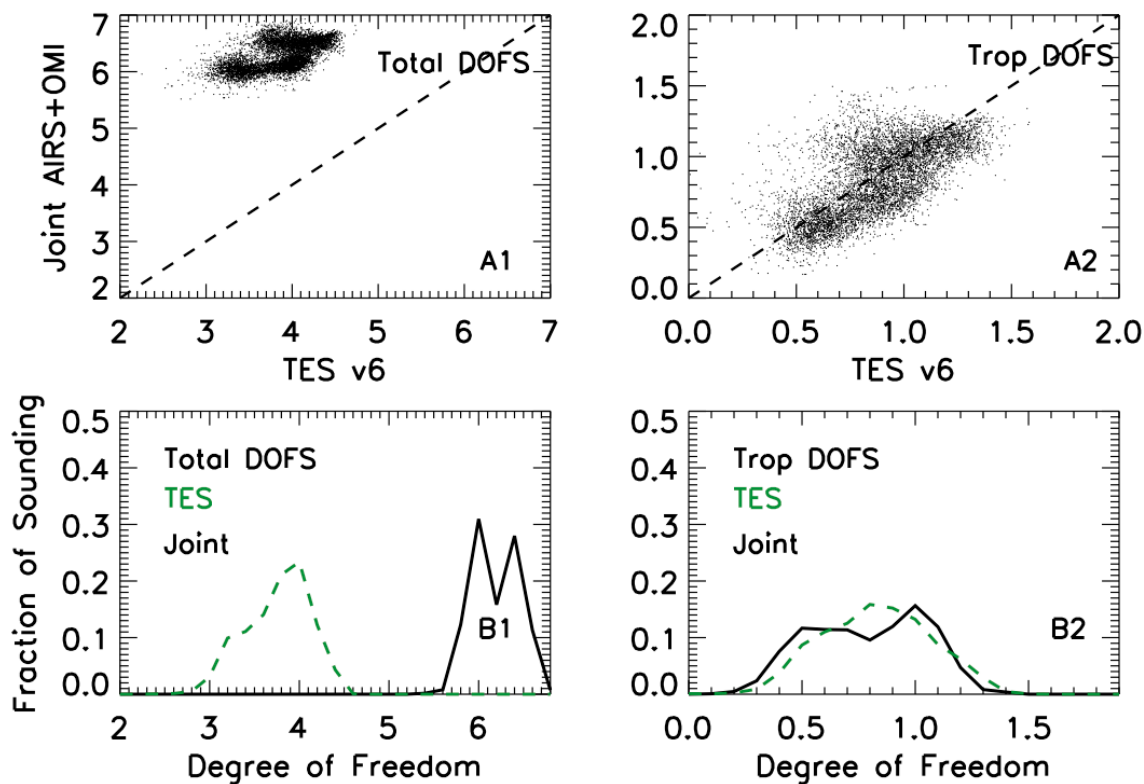


Figure S15: Degree of freedom of signals (DOFS) for April 2006 monthly mean O_3 over globe shown in Fig. S4. (A1) total DOFS; (A2) tropospheric DOFS; and (B1) histogram of total DOFS: joint AIRS+OMI (black line) and TES version 6 (green dash); (B2) histogram of tropospheric DOFS joint AIRS+OMI (black line) and TES version 6 (green dash).

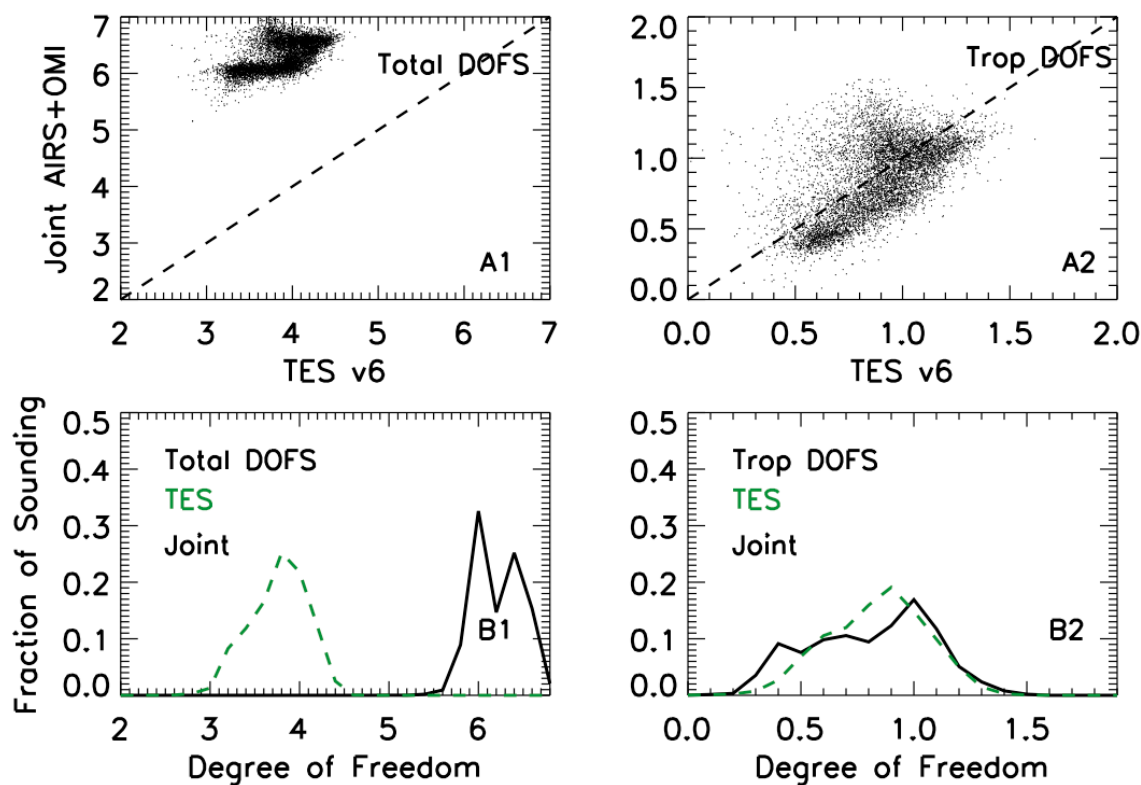


Figure S16: Degree of freedom of signals (DOFS) for May 2006 monthly mean O_3 over globe shown in Fig. S5. (A1) total DOFS; (A2) tropospheric DOFS; and (B1) histogram of total DOFS: joint AIRS+OMI (black line) and TES version 6 (green dash); (B2) histogram of tropospheric DOFS joint AIRS+OMI (black line) and TES version 6 (green dash).

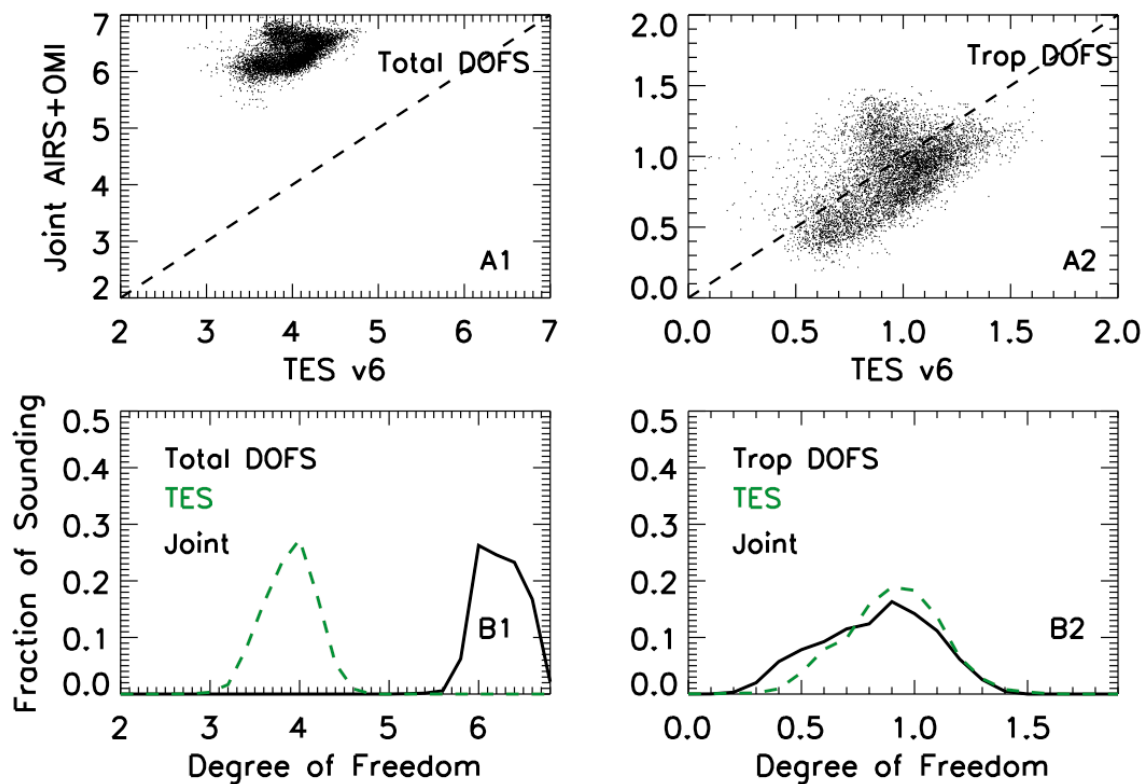


Figure S17: Degree of freedom of signals (DOFS) for June 2006 monthly mean O_3 over globe shown in Fig. S6. (A1) total DOFS; (A2) tropospheric DOFS; and (B1) histogram of total DOFS: joint AIRS+OMI (black line) and TES version 6 (green dash); (B2) histogram of tropospheric DOFS joint AIRS+OMI (black line) and TES version 6 (green dash).

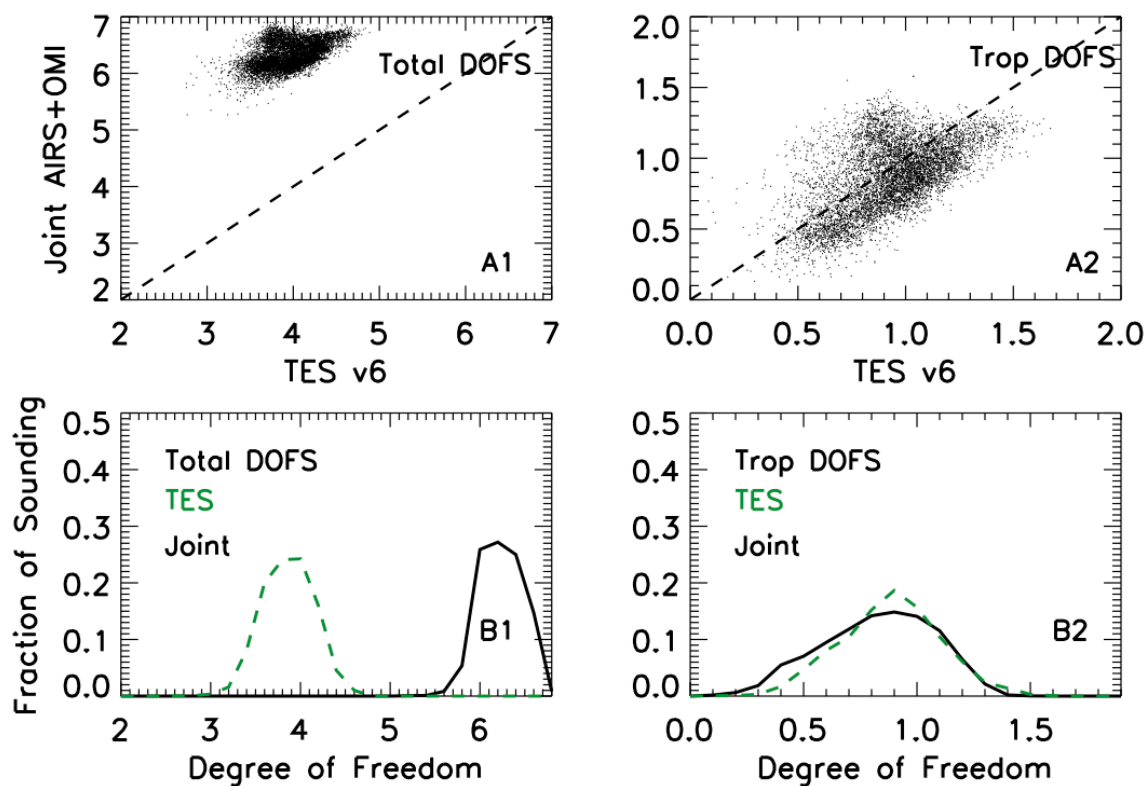


Figure S18: Degree of freedom of signals (DOFS) for July 2006 monthly mean O_3 over globe shown in Fig. S7. (A1) total DOFS; (A2) tropospheric DOFS; and (B1) histogram of total DOFS: joint AIRS+OMI (black line) and TES version 6 (green dash); (B2) histogram of tropospheric DOFS joint AIRS+OMI (black line) and TES version 6 (green dash).

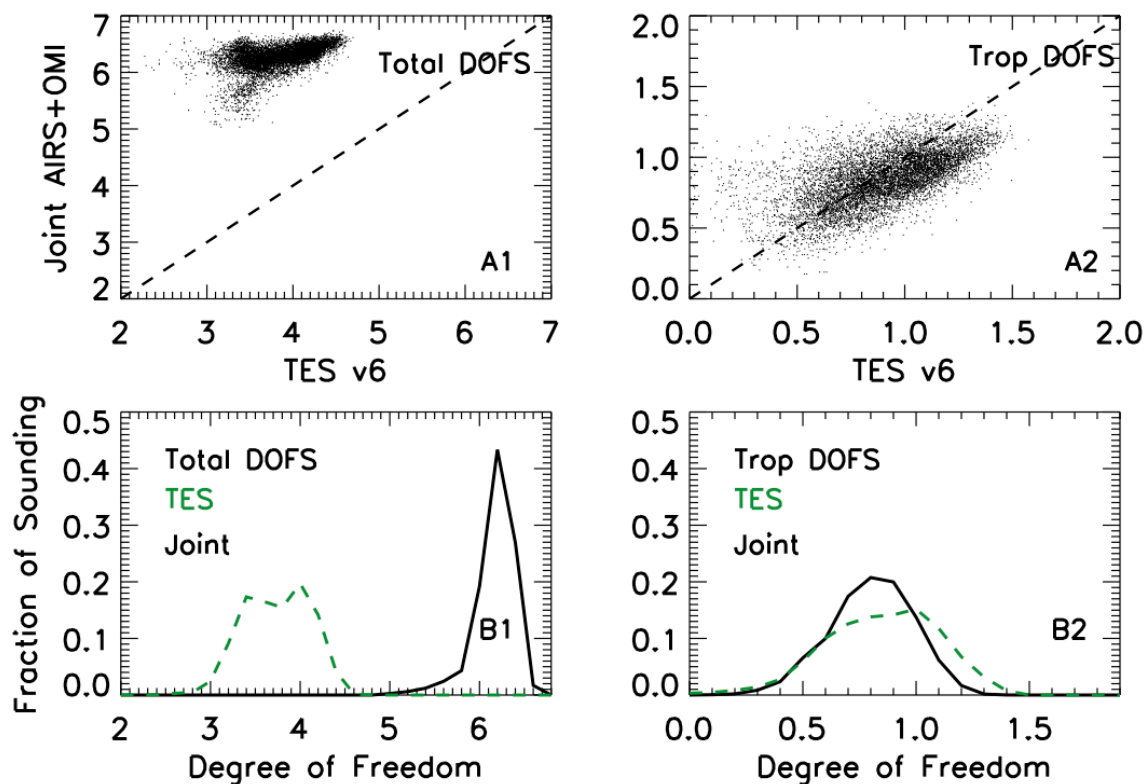


Figure S19: Degree of freedom of signals (DOFS) for September 2006 monthly mean O_3 over globe shown in Fig. S8. (A1) total DOFS; (A2) tropospheric DOFS; and (B1) histogram of total DOFS: joint AIRS+OMI (black line) and TES version 6 (green dash); (B2) histogram of tropospheric DOFS joint AIRS+OMI (black line) and TES version 6 (green dash).

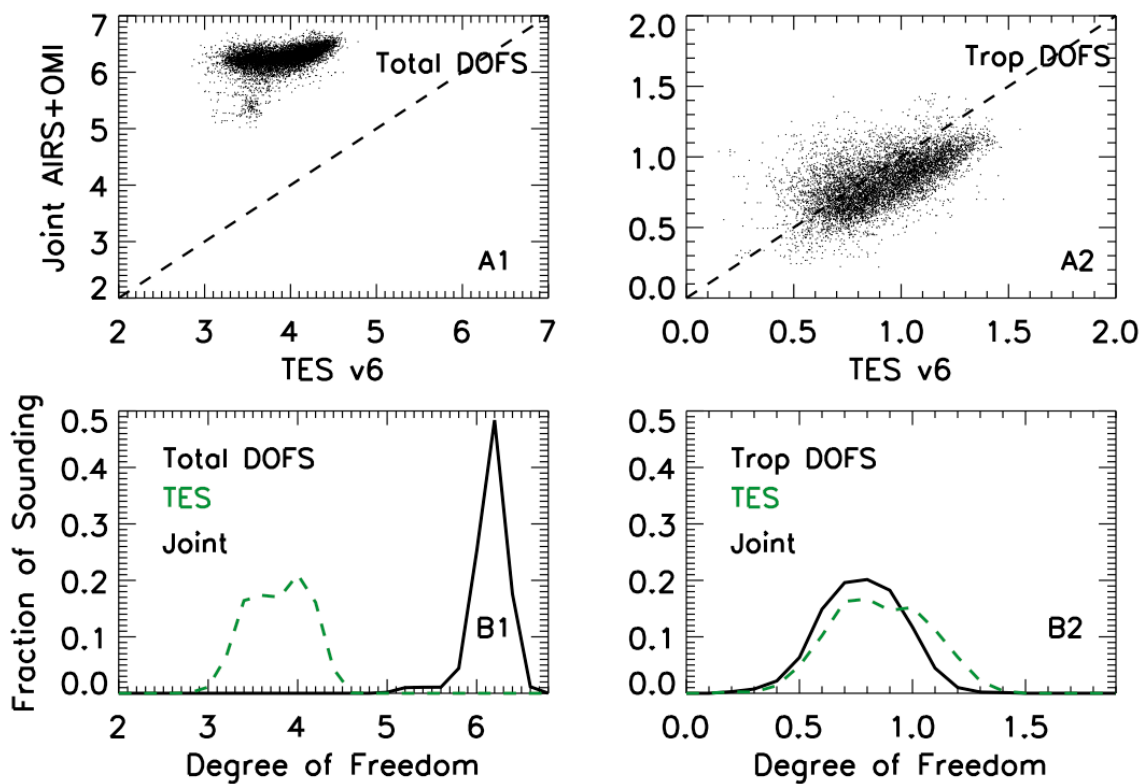


Figure S20: Degree of freedom of signals (DOFS) for October 2006 monthly mean O_3 over globe shown in Fig. S9. (A1) total DOFS; (A2) tropospheric DOFS; and (B1) histogram of total DOFS: joint AIRS+OMI (black line) and TES version 6 (green dash); (B2) histogram of tropospheric DOFS joint AIRS+OMI (black line) and TES version 6 (green dash).

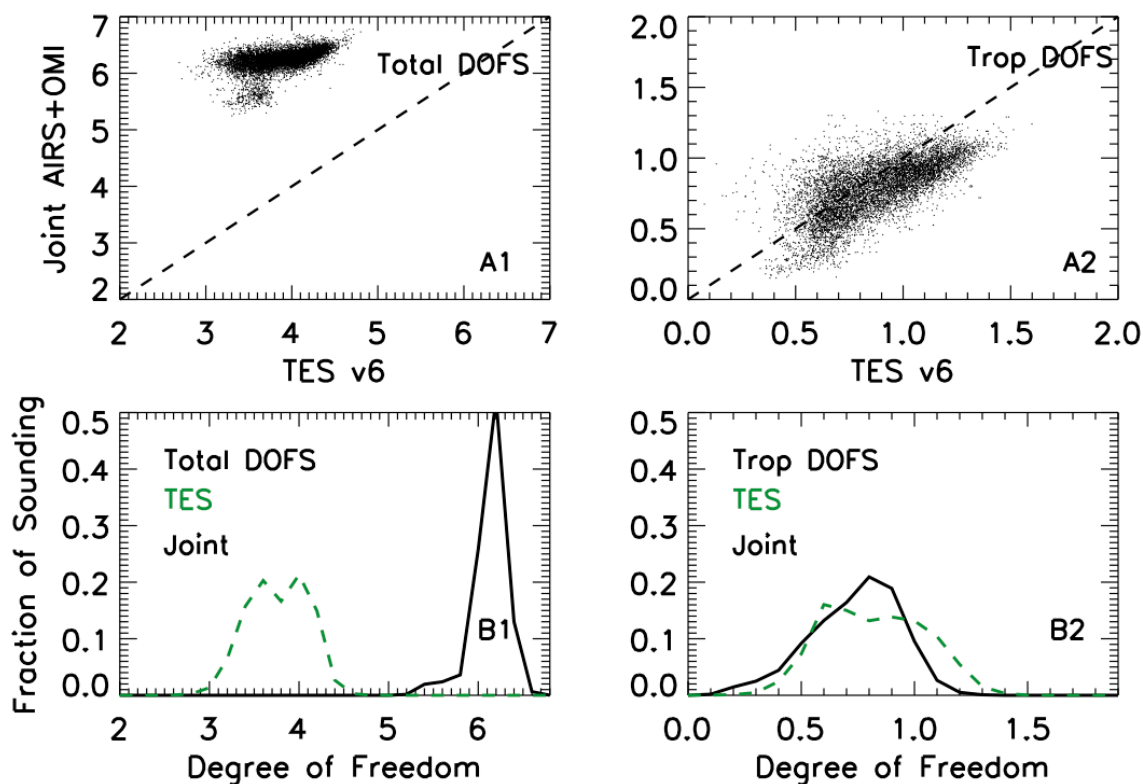


Figure S21: Degree of freedom of signals (DOFS) for November 2006 monthly mean O_3 over globe shown in Fig. S10. (A1) total DOFS; (A2) tropospheric DOFS; and (B1) histogram of total DOFS: joint AIRS+OMI (black line) and TES version 6 (green dash); (B2) histogram of tropospheric DOFS joint AIRS+OMI (black line) and TES version 6 (green dash).

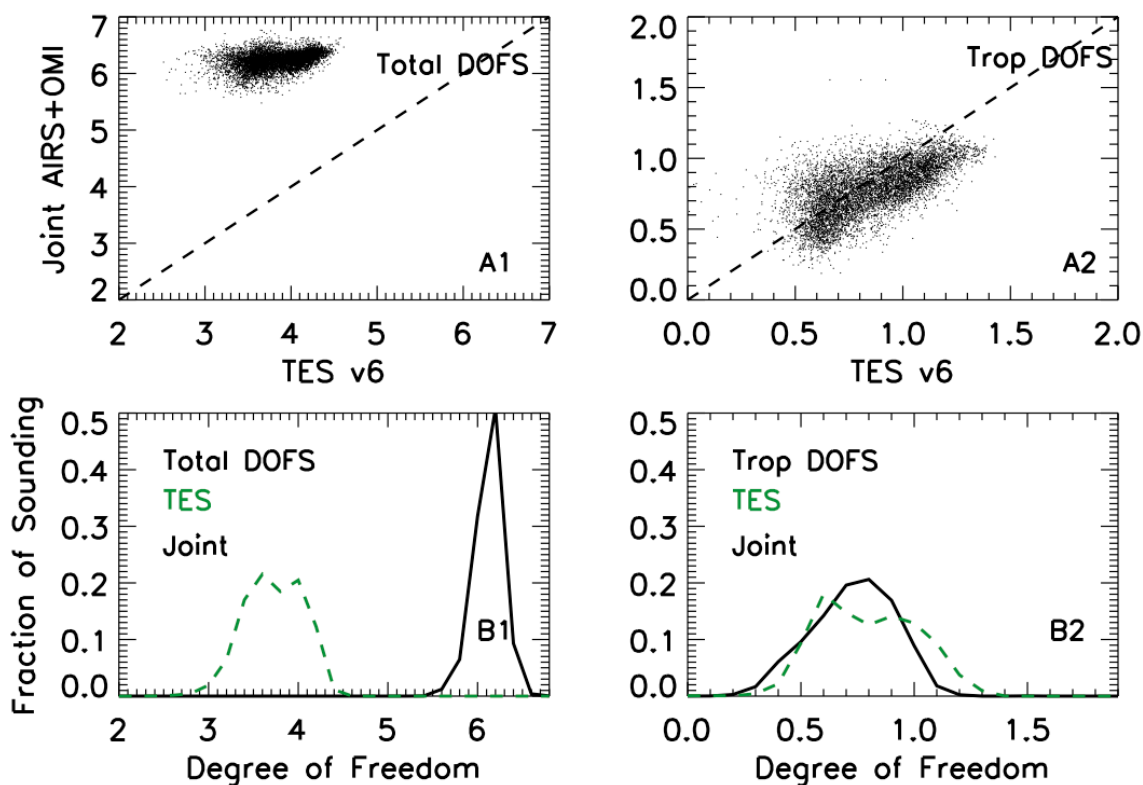


Figure S22: Degree of freedom of signals (DOFS) for December 2006 monthly mean O_3 over globe shown in Fig. S11. (A1) total DOFS; (A2) tropospheric DOFS; and (B1) histogram of total DOFS: joint AIRS+OMI (black line) and TES version 6 (green dash); (B2) histogram of tropospheric DOFS joint AIRS+OMI (black line) and TES version 6 (green dash).

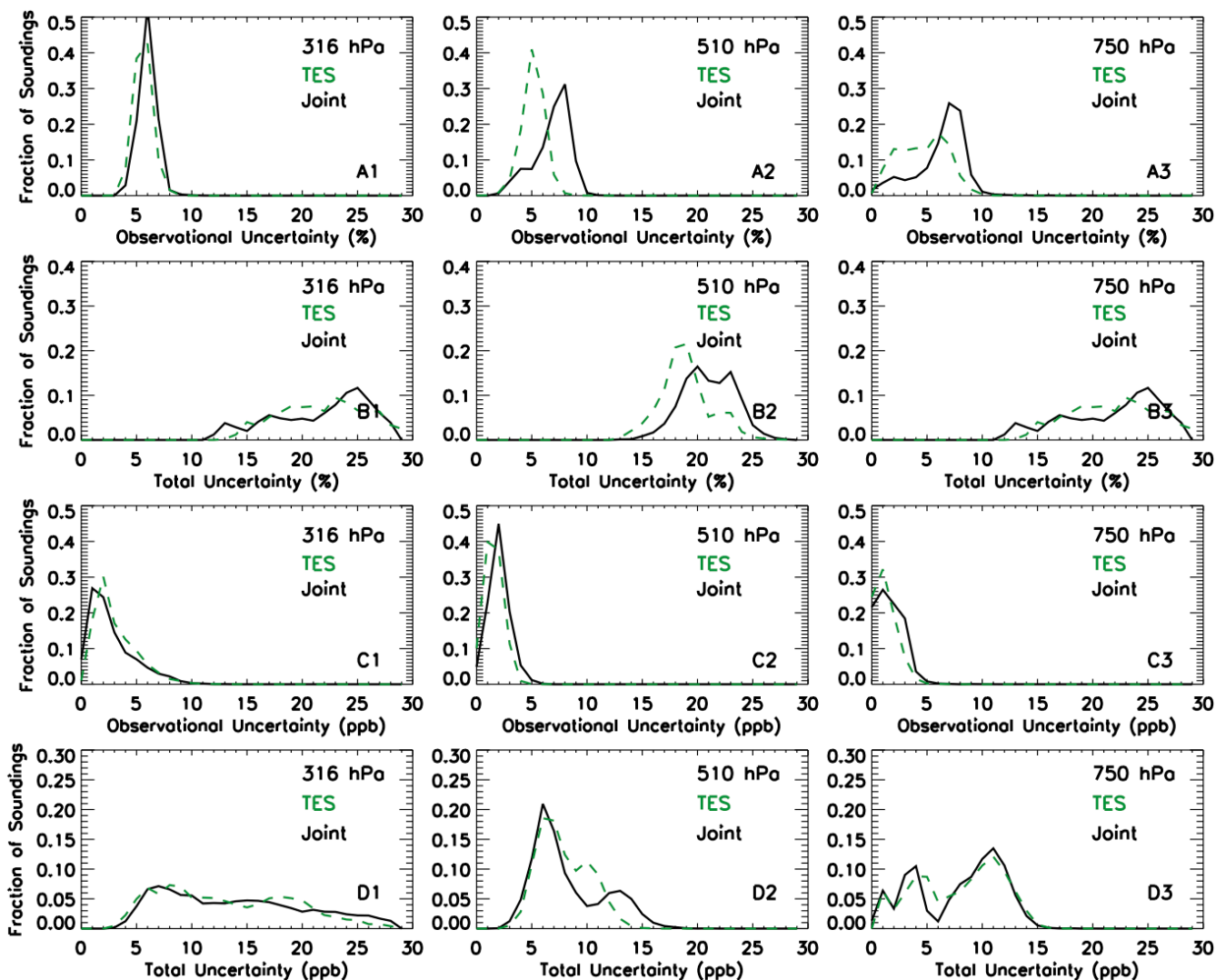


Figure S23: Estimated error of retrieved global O₃ concentration for January 2006 shown in Fig. S1. (A1–A3) observational error; (B1–B3) total error; (C1–C3) observational error in ppb; (D1–D3) total error in ppb. Joint AIRS+OMI data are shown in black line, and TES version 6 data are shown in green dash.

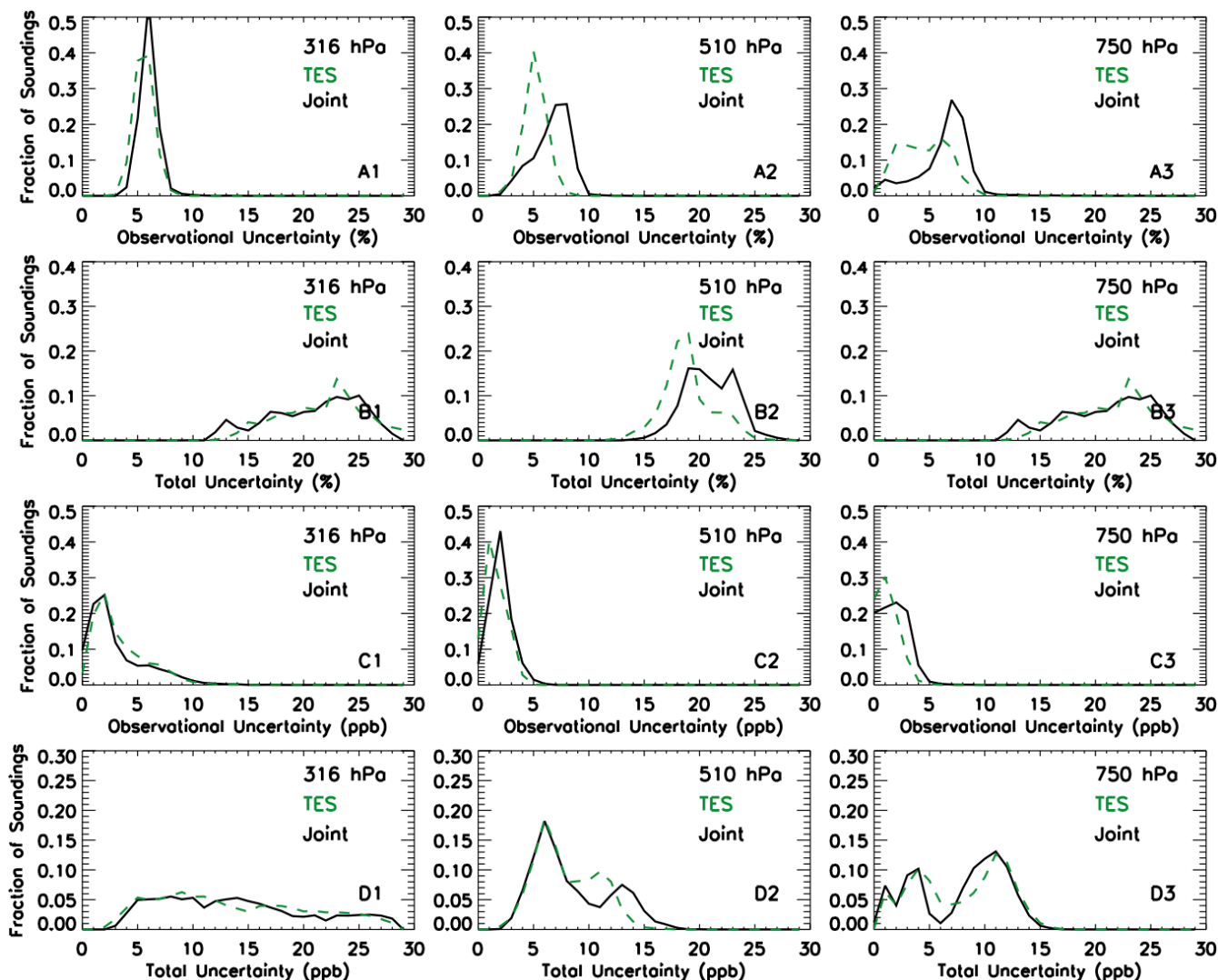


Figure S24: Estimated error of retrieved global O_3 concentration for February 2006 shown in Fig. S2. (A1–A3) observational error; (B1–B3) total error; (C1–C3) observational error in ppb; (D1–D3) total error in ppb. Joint AIRS+OMI data are shown in black line, and TES version 6 data are shown in green dash.

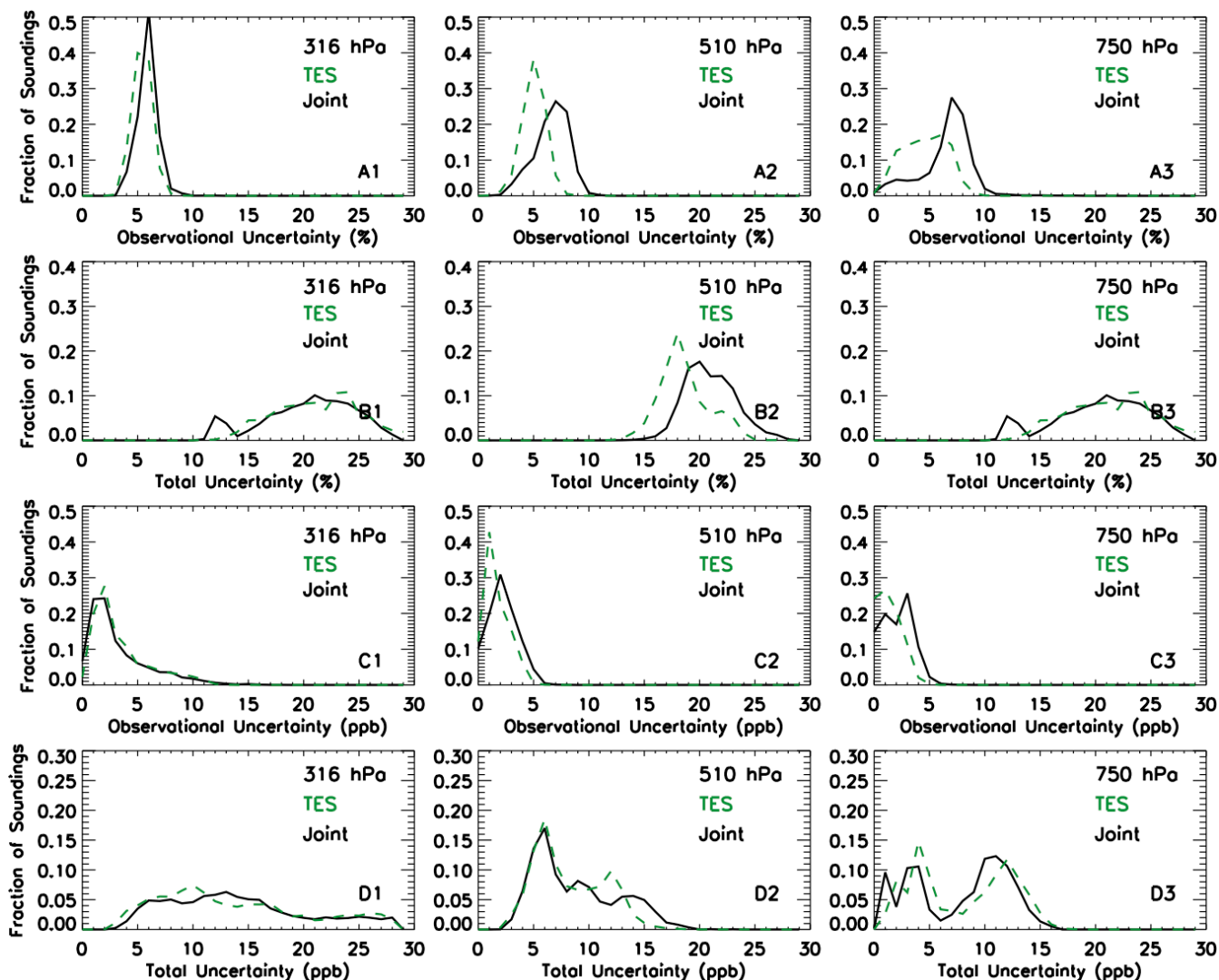


Figure S25: Estimated error of retrieved global O₃ concentration for March 2006 shown in Fig. S3. (A1–A3) observational error; (B1–B3) total error; (C1–C3) observational error in ppb; (D1–D3) total error in ppb. Joint AIRS+OMI data are shown in black line, and TES version 6 data are shown in green dash.

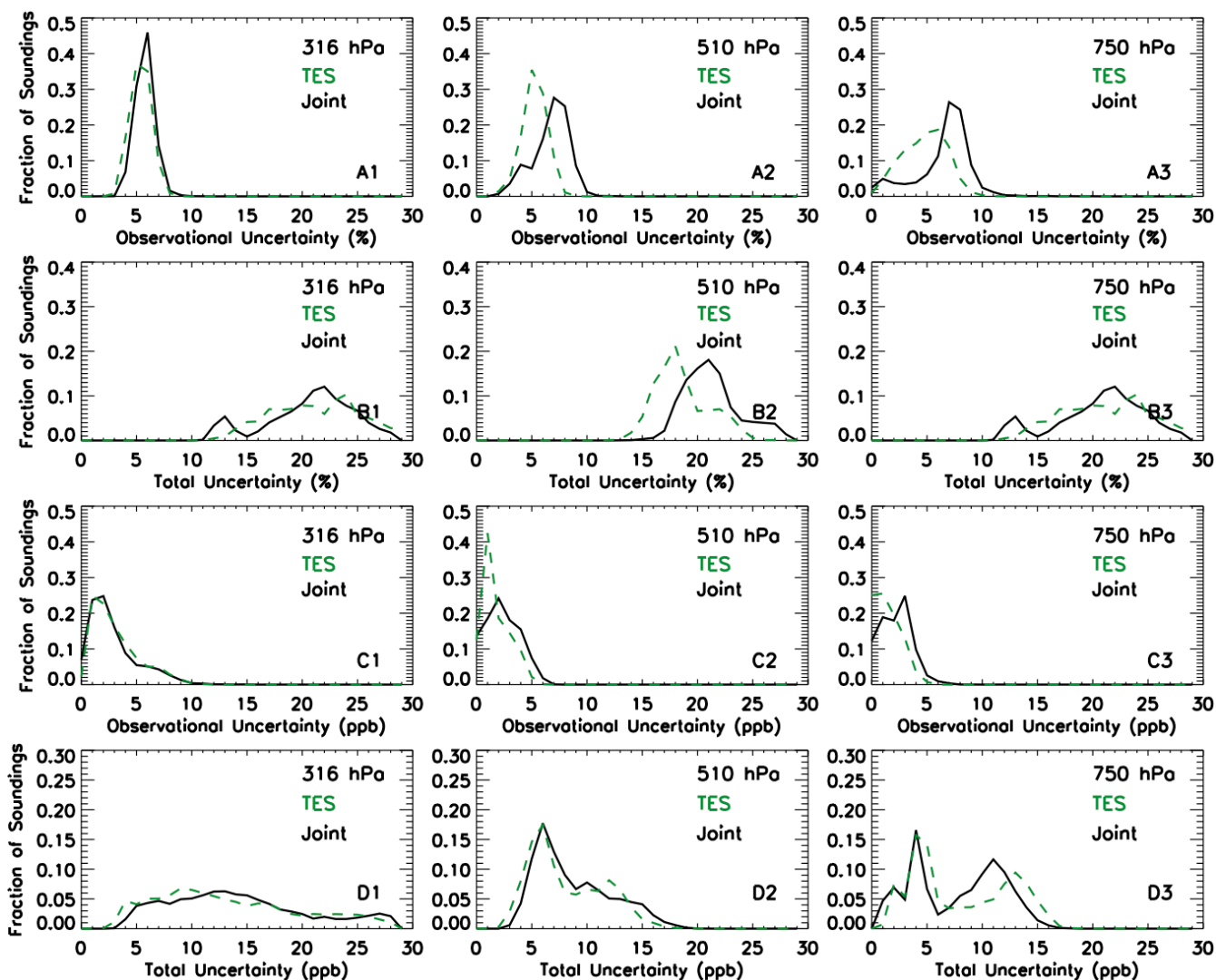


Figure S26: Estimated error of retrieved global O₃ concentration for April 2006 shown in Fig. S4. (A1–A3) observational error; (B1–B3) total error; (C1–C3) observational error in ppb; (D1–D3) total error in ppb. Joint AIRS+OMI data are shown in black line, and TES version 6 data are shown in green dash.

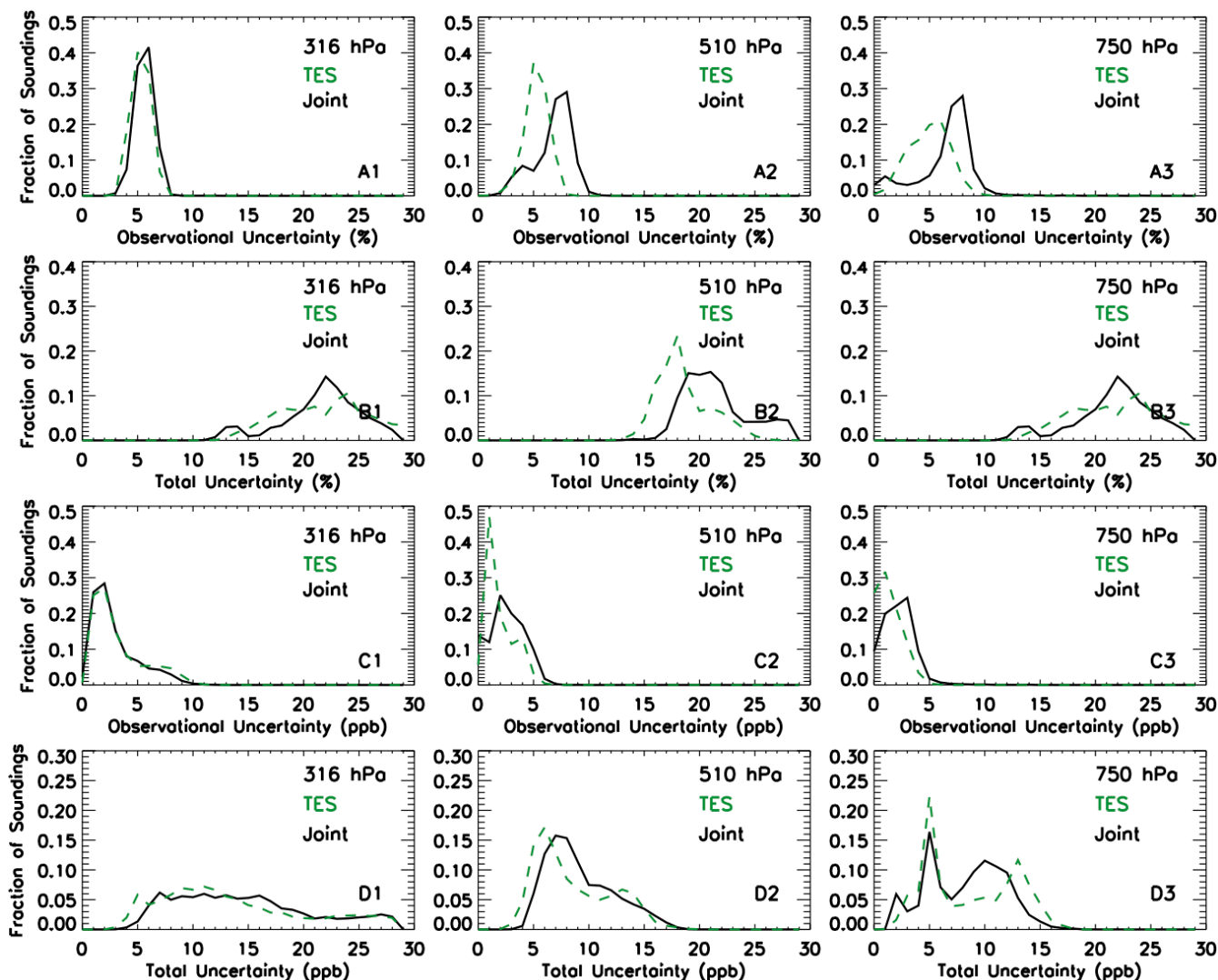


Figure S27: Estimated error of retrieved global O_3 concentration for May 2006 shown in Fig. S5. (A1–A3) observational error; (B1–B3) total error; (C1–C3) observational error in ppb; (D1–D3) total error in ppb. Joint AIRS+OMI data are shown in black line, and TES version 6 data are shown in green dash.

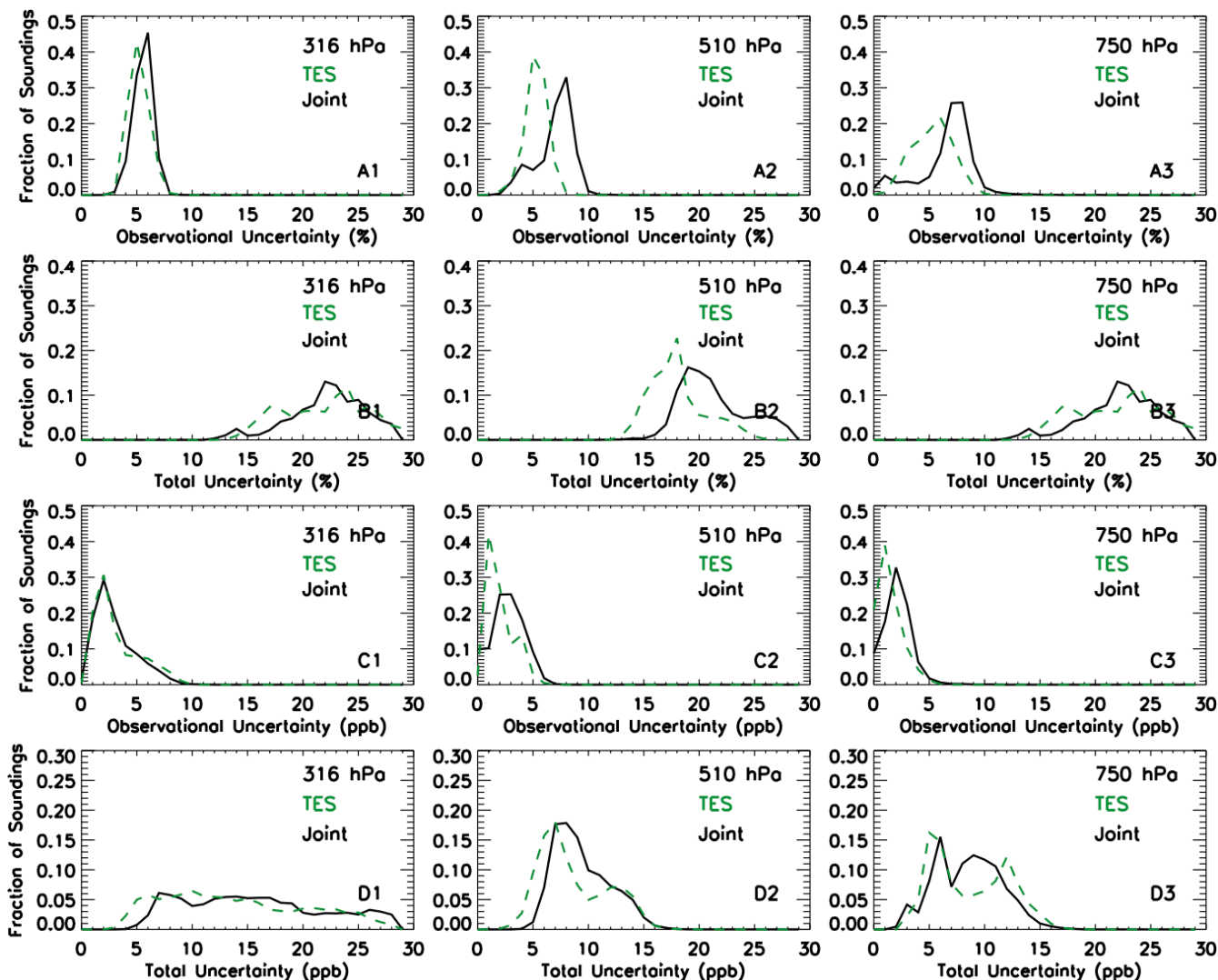


Figure S28: Estimated error of retrieved global O₃ concentration for June 2006 shown in Fig. S6. (A1–A3) observational error; (B1–B3) total error; (C1–C3) observational error in ppb; (D1–D3) total error in ppb. Joint AIRS+OMI data are shown in black line, and TES version 6 data are shown in green dash.

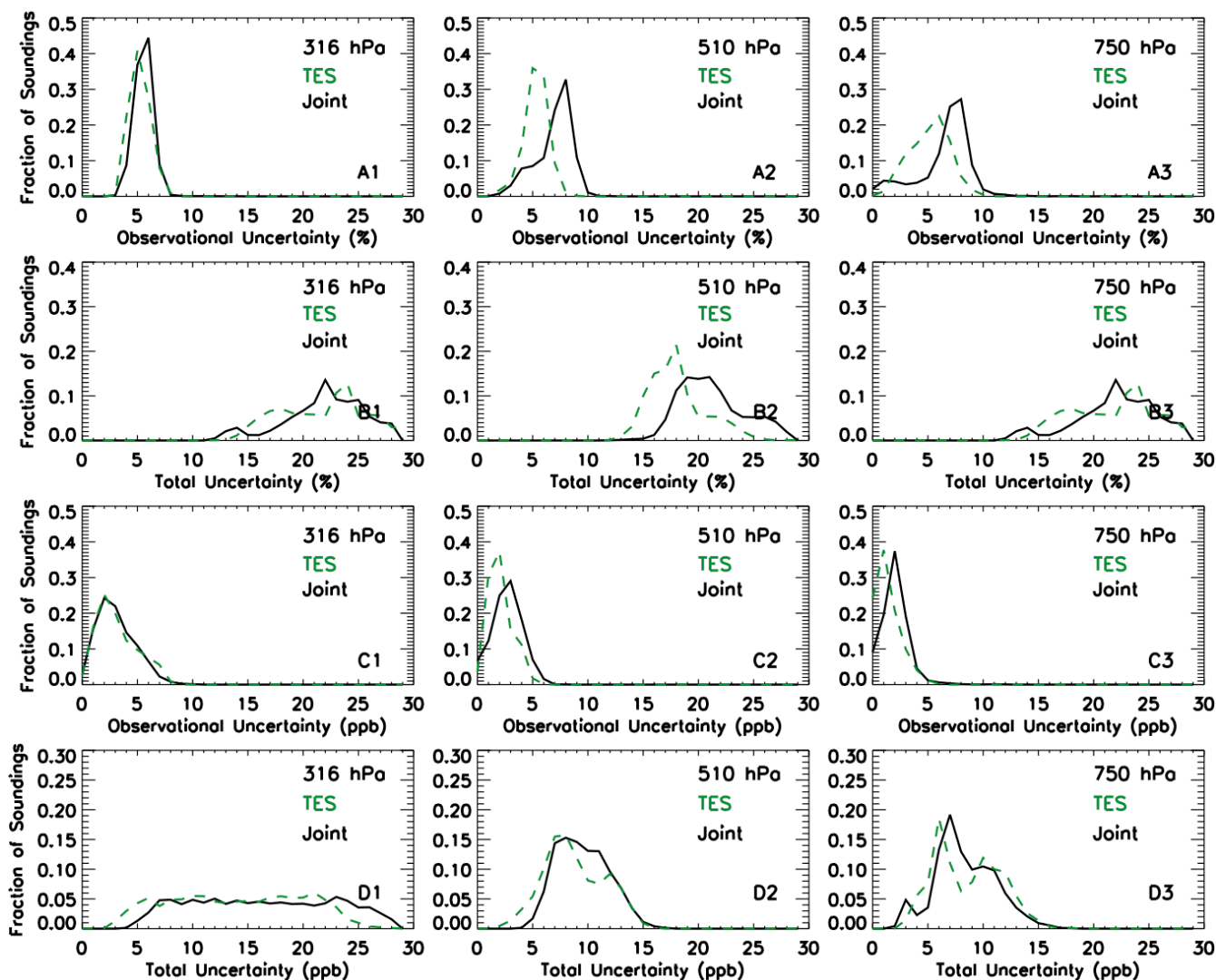


Figure S29: Estimated error of retrieved global O_3 concentration for July 2006 shown in Fig. S7. (A1–A3) observational error; (B1–B3) total error; (C1–C3) observational error in ppb; (D1–D3) total error in ppb. Joint AIRS+OMI data are shown in black line, and TES version 6 data are shown in green dash.

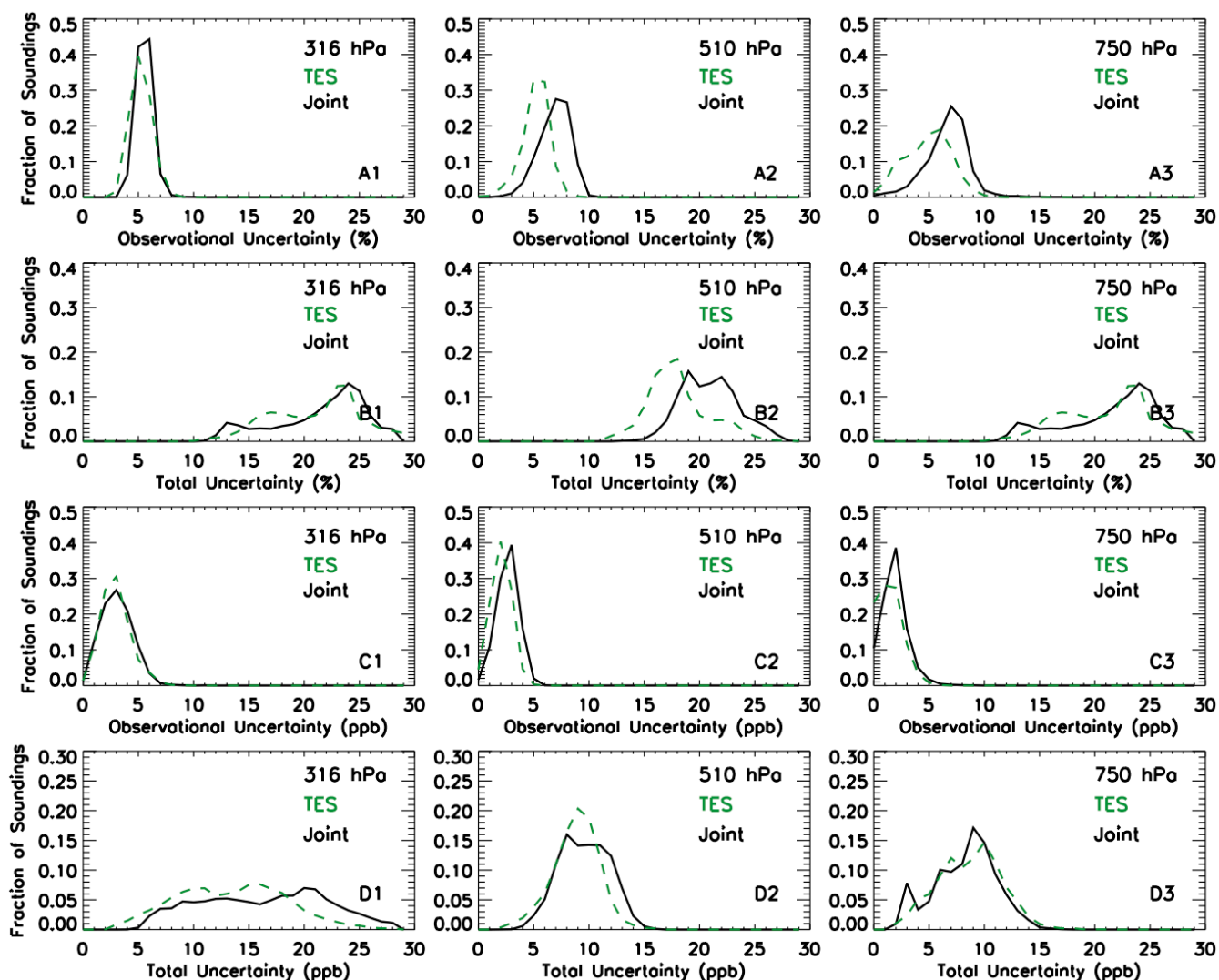


Figure S30: Estimated error of retrieved global O_3 concentration for September 2006 shown in Fig. S8. (A1–A3) observational error; (B1–B3) total error; (C1–C3) observational error in ppb; (D1–D3) total error in ppb. Joint AIRS+OMI data are shown in black line, and TES version 6 data are shown in green dash.

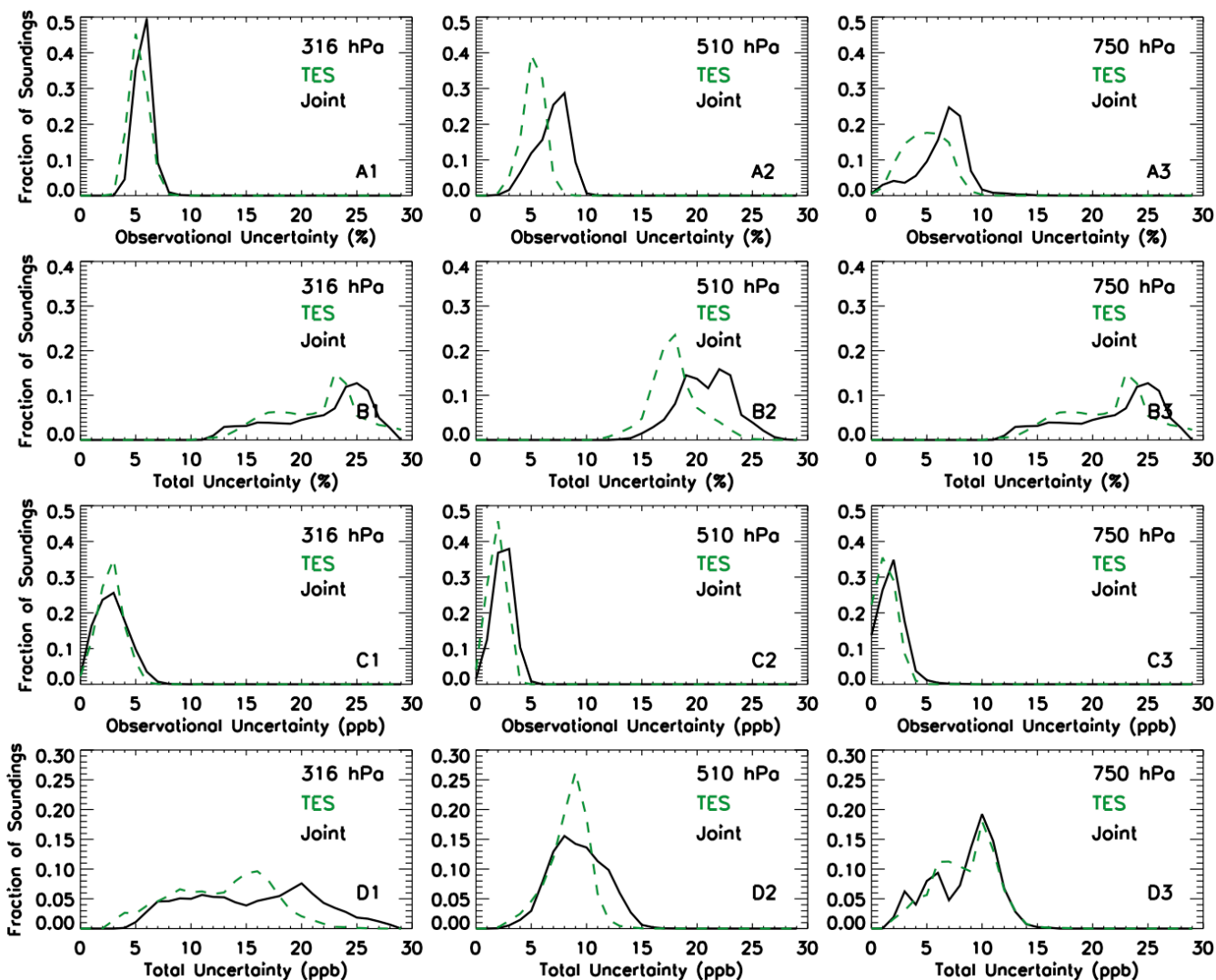


Figure S31: Estimated error of retrieved global O₃ concentration for October 2006 shown in Fig. S9. (A1–A3) observational error; (B1–B3) total error; (C1–C3) observational error in ppb; (D1–D3) total error in ppb. Joint AIRS+OMI data are shown in black line, and TES version 6 data are shown in green dash.

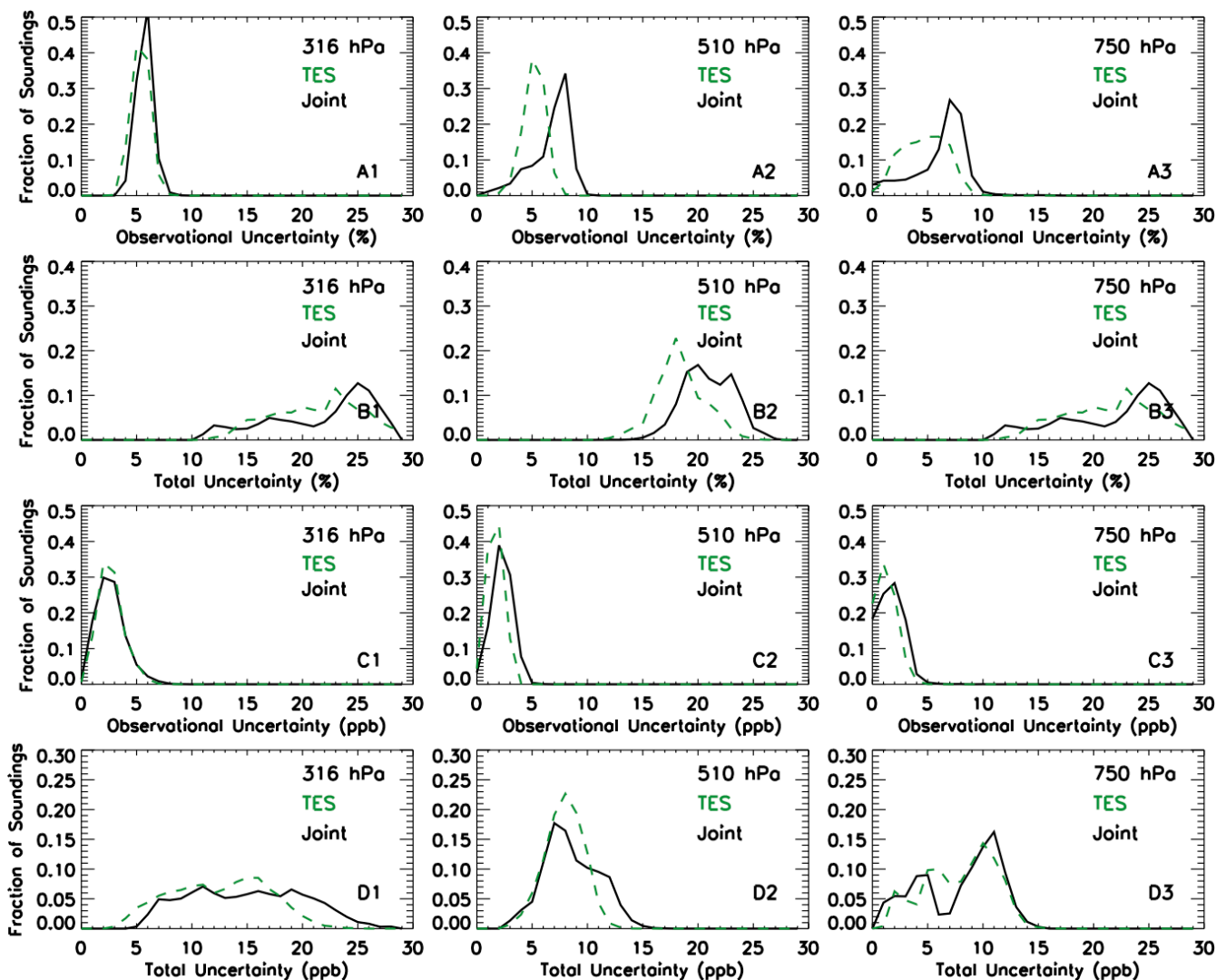


Figure S32: Estimated error of retrieved global O₃ concentration for November 2006 shown in Fig. S10. (A1–A3) observational error; (B1–B3) total error; (C1–C3) observational error in ppb; (D1–D3) total error in ppb. Joint AIRS+OMI data are shown in black line, and TES version 6 data are shown in green dash.

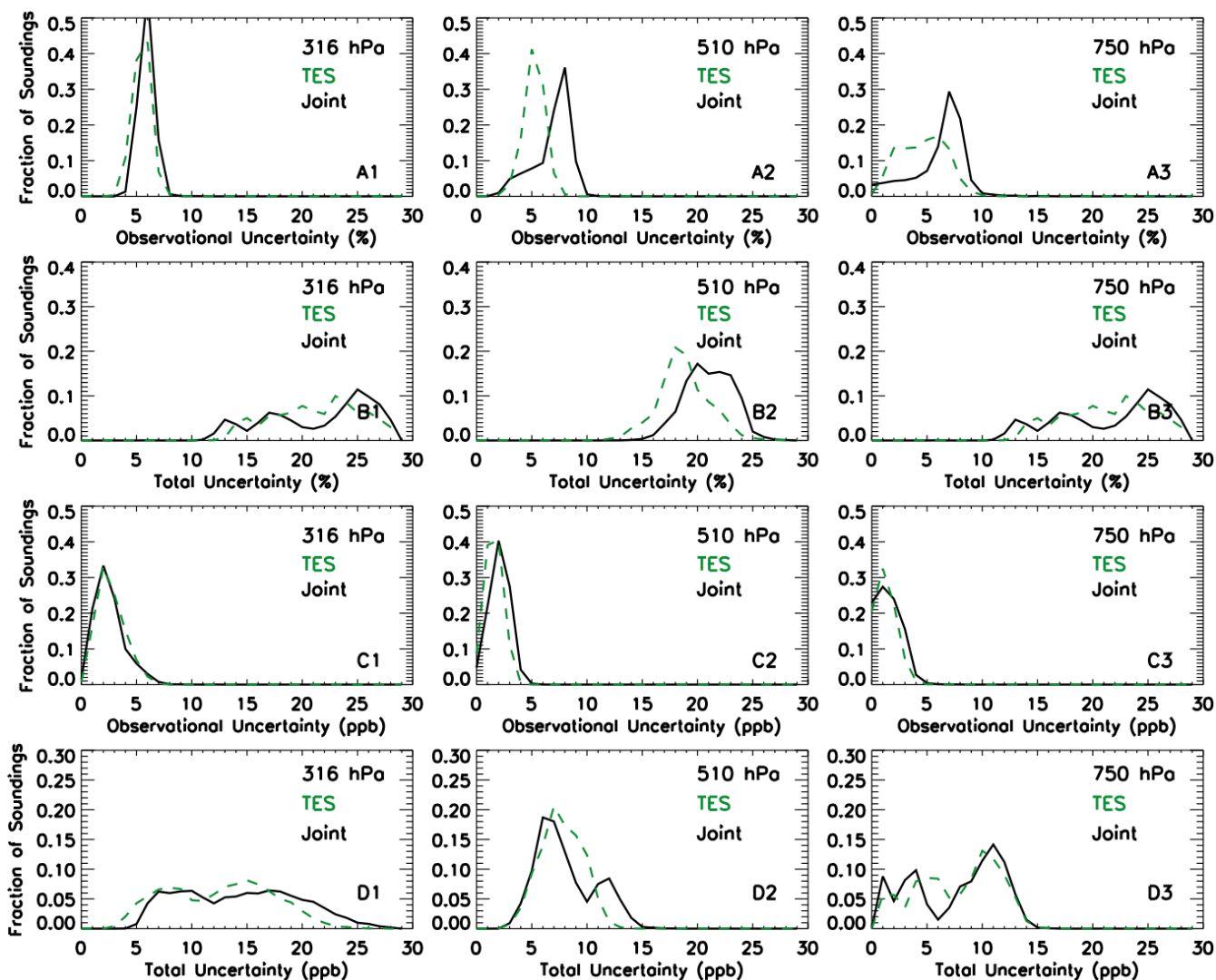


Figure S33: Estimated error of retrieved global O_3 concentration for December 2006 shown in Fig. S11. (A1–A3) observational error; (B1–B3) total error; (C1–C3) observational error in ppb; (D1–D3) total error in ppb. Joint AIRS+OMI data are shown in black line, and TES version 6 data are shown in green dash.